Molecular Human Reproduction, Vol.15, No.4 pp. 259–267, 2009
Advanced Access publication on February 14, 2009 doi:10.1093/molehr/gap010

MHR Basic science of reproductive medicine ORIGINAL RESEARCH

Aberrant DNA methylation status in human uterine leiomyoma

Yoshiaki Yamagata[1], Ryo Maekawa[1], Hiromi Asada[1], Toshiaki Taketani[1], Isao Tamura[1], Hiroshi Tamura[1], Jun Ogane[2], Naka Hattori[3], Kunio Shiota[2], and Norihiro Sugino[1,4]

[1]Department of Obstetrics and Gynecology, Yamaguchi University Graduate School of Medicine, Minamikogushi 1-1-1, Ube 755-8505, Japan [2]Laboratory of Cellular Biochemistry, Animal Resources/Veterinary Medical Science, The University of Tokyo, Bunkyo-ku, Tokyo 113-8657, Japan [3]Institute of Life Science, Ajinomoto Co., INC, 1-1 Suzuki-cho, Kawasaki-ku, Kawasaki 210-8680, Japan

[4]Correspondence address. Tel: +81-836-22-2286; Fax: +81-836-22-2287; E-mail: sugino@yamaguchi-u.ac.jp

ABSTRACT: Aberrant DNA methylation has been implicated in tumorigenesis. This study was undertaken to establish the genome-wide DNA methylation profile in uterine leiomyomas and to investigate whether DNA methylation status is altered in uterine leiomyomas. For this purpose, restriction landmark genomic scanning (RLGS) was performed on a paired sample of leiomyoma and adjacent normal myometrium. The RLGS profile revealed 29 aberrant methylation spots (10 methylated and 19 demethylated) in leiomyoma in comparison with myometrium. One of the differently methylated genomic loci was newly identified as GS20656 from the human genome sequence database. In 9 of the 10 paired samples, the DNA methylation levels of the first exon of GS20656 were significantly lower in leiomyoma than in myometrium, suggesting the existence of a genomic locus under epigenetic regulation in uterine leiomyomas. Unexpectedly, DNA methyltransferase 1 (DNMT1) and DNMT3a mRNA expression levels were higher in leiomyoma than in myometrium. These facts suggest that other epigenetic factors besides DNMT are involved in local changes of DNA methylation at genome loci. The present study indicates not only aberrant genome-wide DNA methylation status in uterine leiomyomas but also the existence of a genomic locus that is differently methylated between normal myometrium and uterine leiomyoma.

Key words: RLGS / DNA methylation / leiomyoma

Introduction

Uterine leiomyomas are the most common tumors in the female genital tract. Approximately 20–25% of women of reproductive age are afflicted with this disease (Vollenhoven *et al.*, 1990). Uterine leiomyomas cause hypermenorrhea, infertility, miscarriage, etc. and in some cases uterine leiomyomas severely affect a woman's daily life. Despite the high prevalence rate and distressing effect on reproductive women, the pathogenesis of uterine leiomyomas remains unclear. Women with African origin, high body mass index, early menarche, hypertension, history of pelvic inflammatory disease and meat intake, etc. are at greater risk for uterine leiomyoma, whereas women with contraceptive use, smoking, parous and green vegetables intake are at lower risk (Chiaffarino *et al.*, 1999; Faerstein *et al.*, 2001a, b; Ryan *et al.*, 2005). These findings suggest that uterine leiomyomas develop not only from inherited genomic abnormalities but also from unfavorable environmental exposure. However, the mechanism of uterine leiomyoma formation and development remains unknown.

Recent microarray analyses have provided much information about mRNA expression in uterine leiomyomas and normal myometrium (Tsibris *et al.*, 2002; Ahn *et al.*, 2003; Wang *et al.*, 2003; Weston *et al.*, 2003; Catherino *et al.*, 2004). Epigenetic mechanisms including DNA methylation and histone modification are known to play key roles in transcriptional regulation. DNA methylation is involved in various developmental processes through the silencing, switching and stabilizing of genes (Li, 2002; Shiota and Yanagimachi, 2002; Shiota, 2004). Aberrant DNA methylation has also attracted researchers' attention in the study of the mechanism of tumorigenesis. Abnormal DNA methylation of the key gene known as a tumor suppressor is involved in carcinogenesis (Ushijima and Okochi-Tanaka, 2005). Interestingly, global hypomethylation and imbalanced expression of DNA methyltransferases (DNMT), which add a methyl group to the cytosine ring to form methyl cytosine (Smith, 1994), were found in uterine leiomyomas (Li *et al.*, 2003). Furthermore, we recently found aberrant DNA methylation at estrogen receptor-α (ER-α) in uterine leiomyomas (Asada *et al.*, 2008), which suggests that epigenetic alteration of the ER-α gene is involved in their pathogenesis. Therefore, a study of both epigenetics and DNA methylation-dependent gene regulation are now essential for investigating the molecular mechanisms involved in the formation and development of uterine leiomyomas.

© The Author 2009. Published by Oxford University Press on behalf of the European Society of Human Reproduction and Embryology. All rights reserved.
For Permissions, please email: journals.permissions@oxfordjournals.org

DNA methylation at the CpG dinucleotides is catalyzed by DNMT. Several DNMTs exist. DNMT1 is responsible for accurately replicating genomic DNA methylation patterns during cell division in mammalian cells (Liu *et al.*, 1998). On the other hand, DNMT3a and DNMT3b are thought to catalyze *de novo* methylation of DNA (Hsieh, 1999). DNMT1, DNMT3a and DNMT3b have also been shown to cooperatively maintain DNA methylation (Ting *et al.*, 2004).

Because mammalian genomes have numerous tissue-dependent differentially methylated regions (T-DMRs) and developmental processes are associated with changes of epigenetics in genome-wide T-DMRs (Cho *et al.*, 2001; Imamura *et al.*, 2001; Shiota, 2004), epigenetic abnormalities may be present in uterine leiomyomas. To date, genome-wide DNA methylation has not been compared between normal myometrium and uterine leiomyoma tissue. The present study was, therefore, undertaken to establish the genome-wide DNA methylation profile of uterine leiomyomas.

Materials and Methods

This study was reviewed and approved by the Institutional Review Board of Yamaguchi University Graduate School of Medicine. Informed consent was obtained from the women before collection of any samples for this study.

Tissue samples

Specimens of uterine leiomyoma and corresponding normal myometrium were obtained from 20 premenopausal women, from 37 to 53 (mean 47.2) years of age, who underwent total hysterectomy. All patients were Japanese. The profile of the samples used in this study is shown in Table 1. Women who had other gynecological diseases were excluded. Tissues were taken immediately after removal of the uterus, immersed in liquid nitrogen and stored at −80°C until further processing. Tissue sections of each sample were examined under light microscopy after hematoxylin and eosin staining to confirm the pathologic nature of the sample.

Restriction landmark genomic scanning

Restriction landmark genomic scanning (RLGS) was performed on a paired sample of uterine leiomyoma and adjacent normal myometrium (Case 1 in Table 1) for screening genome-wide DNA methylation status. Genomic DNA was extracted from the tissues, and RLGS was performed as described previously using the combination of restriction enzymes, NotI–PvuII–PstI (Shiota *et al.*, 2002; Kremenskoy *et al.*, 2003; Hattori *et al.*, 2004a). To block non-specific labeling, genomic DNA was treated with Klenow fragment (TAKARA, Otsu, Japan) in the presence of dGTP, dCTP, ddATP and ddTTP (TAKARA). DNA was digested with NotI as a landmark enzyme (Nippongene, Toyama, Japan), and the resulting cohesive ends were labeled with Sequenase version 2.0 (USB, NE, USA) in the presence of [α-^{32}P]dCTP and [α-^{32}P]dGTP (Amersham-Pharmacia, Buckinghamshire, UK), digested with PvuII (Nippongene) and then subjected to the first dimension electrophoresis in a 0.9% agarose disc gel for 23 h at 230 V. After the DNA fragments were treated with PstI (Nippongene) in the disc gel, the resulting DNA fragments were separated in second dimensional 5% polyacrylamide gel for 20 h at 150 V. The gel was dried onto chromatography paper (Whatman, Maidstone, UK) and exposed to X-ray film (Kodak, XAR5, Eastman Kodak, NY) for 2–3 weeks at −80°C. The profiles were replicated at least twice.

Spot identification by virtual image RLGS

To identify sequences on the spot that are differently methylated between leiomyoma and normal myometrium, we applied virtual image RLGS (vi-RLGS). Vi-RLGS software was developed as reported previously (Matsuyama *et al.*, 2003). The human genome sequence was downloaded in masked FASTA format from the GenBank ftp site and processed with the combination of NotI–PvuII–PstI recognition sequences. We selected candidate loci for intensity-changed spots in 'real' RLGS by matching the vi-RLGS and 'real' RLGS profiles. The corresponding sequences were retrieved by clicking the spot on the virtual image and were used as queries for sequence analysis in Ensembl to obtain the surrounding sequence information. By using the sequence information, the primer sets were designed for methylation-sensitive quantitative real-time PCR as described below.

Table 1 Profile of the samples used in this study

Patients	Age	Location of leiomyoma	Diameter of the leiomyoma (cm)
Case 1	46	Intramural	15
Case 2	50	Intramural	3
Case 3	44	Intramural	8
Case 4	53	Intramural	15
Case 5	49	Intramural	9
Case 6	45	Subserosal	7
Case 7	37	Intramural	8
Case 8	52	Subserosal	9
Case 9	48	Intramural	4
Case 10	48	Subserosal	16
Case 11	50	Subserosal	3
Case 12	49	Intramural	16
Case 13	53	Intramural	7
Case 14	41	Submucosal	5
Case 15	47	Intramural	5
Case 16	48	Submucosal	4
Case 17	48	Intramural	8
Case 18	48	Intramural	6
Case 19	48	Intramural	2
Case 20	46	Submucosal	2

Profiles of the samples used in this study are shown. Cases 1–10 were used for analyses of DNA methylation status of the first exon of GS20656 (Fig. 4A), GS20656 mRNA expression (Fig. 4B) and mRNA expression of DNMT (Fig. 5). Cases 11–20 were used only for analysis of mRNA expression of DNMT.

Methylation analysis based on real-time PCR

Methylation status at several intensity-changed spots detected by RLGS was evaluated by using a combination of the methylation-sensitive restriction digestion and quantitative real-time PCR (Heid *et al.*, 1996). Genomic DNA was digested by PstI, and the aliquot was treated subsequently with NotI. The primer sets for PCR were designed to amplify the region that includes the NotI site detected in RLGS analysis. One hundred nanograms of genomic DNA treated with or without NotI was analyzed by real-time PCR with the primers. The amount of undigested DNA both in NotI-treated and -untreated genomic DNA was estimated by real-time PCR with SYBR premix (TAKARA) by using Light Cycler (Roche, Indianapolis, IN, USA) according to the manufacturer's protocol. The methylation ratio at GENSCAN00000020656 (GS20656) locus, which was conclusively identified as one of the hypomethylated loci in uterine leiomyoma, was

defined according to the proportion of the amount of undigested DNA in NotI-treated genome to that in the NotI-untreated one. The initial DNA amount in the reaction mixture was normalized with RNaseP control reagent (Applied Biosystems, Foster City, CA, USA). For all samples, at least three independent PCR were repeated. Primer sets of GS20656 locus were shown in Table II.

Sodium bisulfite sequencing

Methylation status in the promoter region of the putative gene of GS20656 was investigated using the sodium bisulfite sequencing method. Sodium bisulfite treatment of genomic DNA and sequencing analysis was carried out as reported previously (Hattori *et al.*, 2004b; Asada *et al.*, 2008). Briefly, 2 μg of genomic DNA was digested with NsiI, denatured by adding 0.3 M of NaOH and incubated for 20 min at 42°C. After incubation, sodium metabisulfite (pH 5.0) and hydroquinone were added to final concentrations of 2.0 M and 0.5 mM, respectively, and the mixture was further incubated in the dark for 16 h at 55°C. The modified DNA was purified with a Wizard DNA Clean-Up system (Promega, Madison, WI, USA), and the bisulfite reaction was terminated with NaOH at a final concentration of 0.3 M for 20 min at 42°C. The solution was then neutralized by adding NH_4OAc (pH 7.0) to a final concentration of 3 M. The ethanol-precipitated DNA was resuspended in water, and the DNA fragment covering the putative promoter region and neighboring NotI site region of GS20656 gene was amplified by PCR using the primers shown in Table II. The PCR products were cloned into pGEM-T Easy Vector (Promega), and 10 or more clones randomly picked from each of the two independent PCRs were sequenced to determine the presence of methylated cytosines.

RT–PCR

Total RNA was extracted from paired samples of uterine leiomyoma and normal myometrium using Isogen (Wako, Osaka, Japan), and real-time RT–PCR was performed as reported previously (Asada *et al.*, 2008). RT reactions were performed with ExScript RT reagent kit (TAKARA) according to the manufacturer's protocol. Briefly, 2 μg of total RNA was incubated with 4 μl of 5 × ExScript buffer, 1 μl of dNTP mixture (10 mM each), 1 μl of Random primers (50 μM), 0.5 μl of ExScript RTase (200 U/μl) and 0.5 μl of RNase inhibitor (40 U/μl) in 20 μl of reaction mixture at 42°C for 15 min, after which the reverse transcriptase was inactivated by heating the samples at 95°C for 2 min. The complementary DNA (cDNA) was immediately used for PCR. All PCRs were performed using SYBR Premix Ex *Taq* (TAKARA) and a LightCycler (Roche Applied Science, Basel, Switzerland). Briefly, 2 μl of aliquots containing cDNA were amplified in a total volume of 20 μl containing 4 μl of 5× SYBR PreMix Ex *Taq* and each of primer sets (0.2 μM) described below.

Primer set I was designed in the putative first exon of GS20656 (Fig. 1) for real-time RT–PCR as shown in Table II, corresponding to a 133 bp fragment. To cover a longer region of the first exon of GS20656 than primer set I covers, primer set II (Fig. 1) was designed as shown in Table II and used for RT–PCR, corresponding to a 250 bp fragment. In-line with a previous report (Girault *et al.*, 2003), the primers for DNMT1, DNMT3a and DNMT3b were used for real-time RT–PCR as shown in Table II. For internal controls, TATA box-binding protein (TBP) cDNA or GAPDH cDNA was amplified with each set of primers as shown in Table II. All samples were run in duplicate. Melting curves of the products were obtained after cycling by a stepwise increase of temperature from 55 to 95°C. At the end of 40 cycles, reaction products were separated electrophoretically on an agarose gel and stained with ethidium bromide for visual confirmation of the PCR products.

Statistical analysis

Differences were examined with Student's *t*-test and χ^2 test using the computer program SPSS version 13.0 for Windows. A value of $P < 0.05$ was considered to be significant.

Table II Primers used in the present study

Gene	Primer	Amplification size (bp)	Method
GS20656	F:5′-CCTCTCCGCCTCCCGATGG-3′		Methylation-sensitive
	R:5′-TGATGTGTGTTTGGTGAGCAAGG-3′		quantitative real-time PCR
GS20656	F:5′-GGGGTGGTTAATTTTAGAGATGATT-3′		Sodium bisulfite sequencing
	R:5′-TTACTCTCCAAAACCAAATACCAAA-3′		
GS20656	F:5′-CAGCTGGTCACGTCCTCAC-3′	133	Real-time RT–PCR (primer set I)
	R:5′-CCAAAGGAGAGGCACAAAAG-3′		
GS20656	F:5′-CAGCTGGTCACGTCCTCAC-3′	250	RT–PCR (primer set II)
	R:5′-CAACAATTGCCTCACAATCG-3′		
DNMT1	F:5′-TACCTGGACGACCCTGACCTC-3′	103	Real-time RT–PCR
	R:5′-CGTTGGCATCAAAGATGGACA-3′		
DNMT3a	F:5′-TATTGATGAGCGCACAAGAGAGC-3′	111	Real-time RT–PCR
	R:5′-GGGTGTTCCAGGGTAACATTGAG-3′		
DNMT3b	F:5′-GGCAAGTTCTCCGAGGTCTCTG-3′	113	Real-time RT–PCR
	R:5′-TGGTACATGGCTTTTCGATAGGA-3′		
TBP	F:5′-TGCACAGGAGCCAAGAGTGAA-3′	132	Real-time RT–PCR
	R:5′-CACATCACAGCTCCCCACCA-3′		
GAPDH	F:5′-AGGTGAAGGTCGGAGTCA-3′	99	Real-time RT–PCR
	R:5′-GGTCATTGATGGCAACAA-3′		

F, forward primer; R, reverse primer.

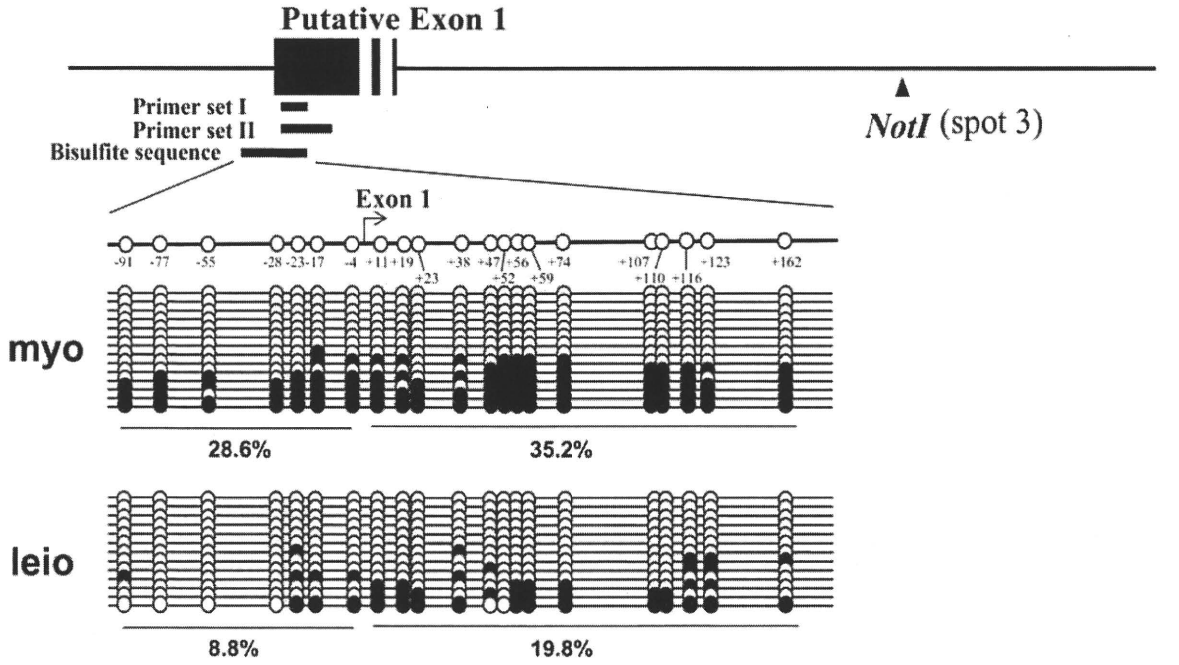

Figure 1 DNA methylation status of the 5'-flanking region of GS20656 in normal myometrium and uterine leiomyoma. The region of the first exon is shown as a thick black bar. The boundary between the first exon and the first intron was blurred. The arrowhead indicates NotI site of the spot #3 in the RLGS profile shown in Fig. 2. The region including the promoter and the first exon (thin black bar) was analyzed by sodium bisulfite sequencing. There are 21 CpG sites between −91 and +162 in the promoter and the first exon regions. Methylation status of the individual CpG site was analyzed in the normal myometrium (myo) and the uterine leiomyoma (leio). Open and closed circles indicate unmethylated and methylated CpG status, respectively.

Results

RLGS analysis

A representative RLGS profile of normal myometrium, consisting of ~1800 spots, is shown in Fig. 2A. In RLGS profiles, the spots are visible if the corresponding NotI site in the genome is unmethylated or hypomethylated, whereas they are invisible if the NotI site is hypermethylated. Numbered circles indicate the 29 spots in which the intensity of spots was either higher or lower than the corresponding spots in the uterine leiomyoma, indicating that there were 29 altered spots in the uterine leiomyoma compared with the normal myometrium. Figure 2B shows the magnified views of the 29 spots. Nineteen spots indicated by the open arrow heads in the leiomyoma were increased in intensities (# 1–3, 8–12, 15–17, 20, 21, 23 and 25) or newly appeared (# 6, 18, 22 and 27) in comparison with the myometrium, indicating that these spots are demethylated or unmethylated in the uterine leiomyoma compared with the normal myometrium. On the other hand, 10 spots indicated by closed arrow heads in the leiomyoma were decreased in intensities (# 4, 7, 26 and 29) or disappeared (# 5, 13, 14, 19, 24 and 28) in comparison with myometrium, suggesting that these spots are hypermethylated or methylated in the uterine leiomyoma compared with the normal myometrium.

Identification of the gene with altered DNA methylation status

The genomic locus of the spot #3 shown in Fig. 2, which is demethylated in the uterine leiomyoma compared with the normal myometrium, was identified using vi-RLGS. Methylation levels at the spot #3 locus in the uterine leiomyoma and normal myometrium were determined by methylation-sensitive quantitative real-time PCR. The methylation level at the spot #3 locus in the uterine leiomyoma (13.4 ± 3.0%) was significantly lower than that in the normal myometrium (52.2 ± 4.2%) (Fig. 3), confirming that this locus is actually hypomethylated in the uterine leiomyoma compared with the normal myometrium. Because the spot #3 locus was not recorded in a known gene coding region in the human genome sequence database, it was considered to be a new putative gene and was named as GS20656 in this study. GS20656 is located in chromosome 15, q23 (AC009434.19.1.177207). Future studies are needed to identify the sequence of other spots that are differently methylated between leiomyoma and normal myometrium.

DNA methylation status of 5'-flanking region of GS20656

The methylation status in the promoter region and the first exon of GS20656 was investigated by sodium bisulfite sequencing (Fig. 1).

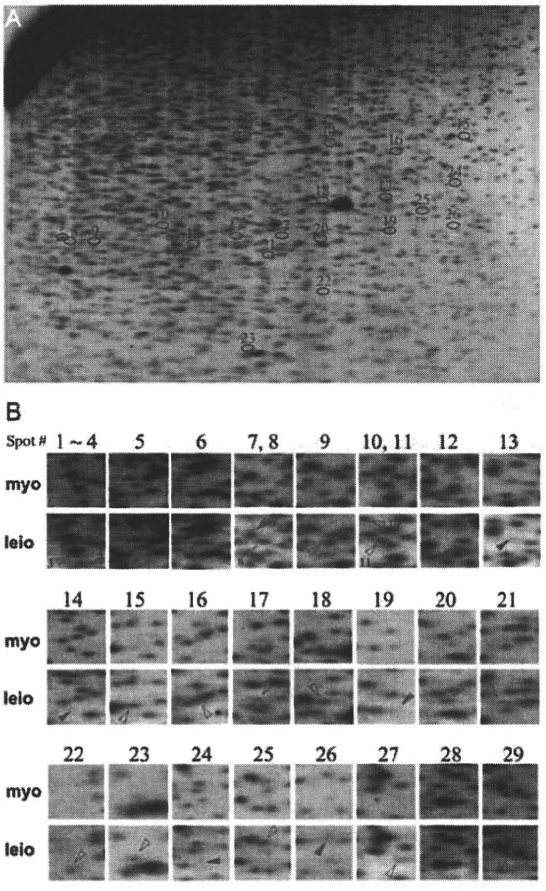

Figure 2 Genome-wide DNA methylation analysis of uterine leiomyoma and the corresponding normal myometrium. (**A**) Representative RLGS profile of a normal myometrium. Numbered circles indicate the 29 spots in which the intensity of spots was either higher or lower than the corresponding spots in the uterine leiomyoma. (**B**) Magnified views of the 29 spots in the uterine leiomyoma (leio) and their adjacent normal myometrium (myo). The spots are visible if the corresponding NotI site in the genome is unmethylated or hypomethylated, whereas they are invisible if the NotI site is hypermethylated. Nineteen spots indicated by open arrow heads in the leiomyoma were increased in intensities (# 1–3, 8–12, 15–17, 20, 21, 23 and 25) or newly appeared (# 6, 18, 22 and 27) in comparison with the myometrium. On the other hand, 10 spots indicated by closed arrow heads in the leiomyoma were decreased in intensities (# 4, 7, 26 and 29) or disappeared (# 5, 13, 14, 19, 24 and 28) in comparison with myometrium.

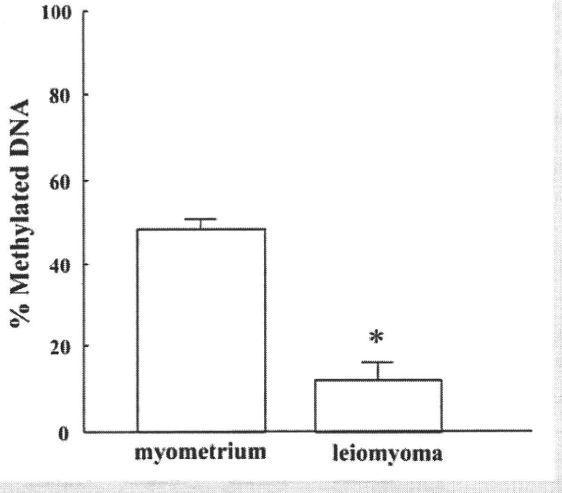

Figure 3 Percentage methylated DNA at the spot #3 locus in the normal myometrium and uterine leiomyoma. DNA methylation levels were determined by methylation-sensitive quantitative real-time RT–PCR as described in the Materials and Methods section. Values are mean + SEM of three different experiments. *$P < 0.05$ versus myometrium (Student's *t*-test).

ı the promoter region examined, only 8 CpGs (8.8%) in a total of 91 xamined CpGs were methylated in the uterine leiomyoma, whereas 8 CpGs (28.6%) in a total 98 examined CpGs were methylated in the ormal myometrium. In the first exon examined, 39 CpGs (19.8%) in a otal of 196 examined CpGs were methylated in the uterine leiomyoma, whereas 64 CpGs (35.2%) in a total 182 examined CpG ites were methylated in the normal myometrium. In both regions, CpGs were significantly hypomethylated in the uterine leiomyoma compared with the normal myometrium ($P < 0.01$, χ^2 test).

Relationship between methylation status and mRNA expression of GS20656

Ten cases (Cases 1–10 in Table I) were analyzed for DNA methylation status and mRNA expression of GS20656. In 9 of the 10 cases examined (all except Case 8), the DNA methylation levels in the first exon of GS20656 were significantly lower in the leiomyoma than in the myometrium (Fig. 4A) ($P < 0.05$, Student's *t*-test). In five of these cases, GS20656 mRNA expression was higher in the leiomyoma than in the myometrium (Fig. 4B).

DNMT mRNA expression

DNMT mRNA expression was examined in the same 10 paired samples as shown in Fig. 4. In 9 of the 10 cases examined (all except Case 1), DNMT1 mRNA expression was higher in the leiomyoma than in the myometrium (Fig. 5A). DNMT3a mRNA expression was higher in the leiomyoma than in the myometrium in all 10 cases (Fig. 5B), whereas DNMT3b mRNA expression was higher in the leiomyoma in only two cases (Fig. 5C). Furthermore, DNMT mRNA expression levels were examined on additional 10 paired samples (Cases 11–20 in Table I), and statistical analysis was performed in 20 cases altogether. DNMT1 and DNMT3a mRNA levels were significantly higher in the leiomyoma than in the myometrium (Table III). In 15 of the 20 cases (75%), DNMT1 mRNA expression was higher in the leiomyoma than in the myometrium, and DNMT3a mRNA expression was higher in the leiomyoma in 17 cases (85%) (Table III). Although DNMT3b mRNA levels tended to be lower in the leiomyoma, the difference was not statistically

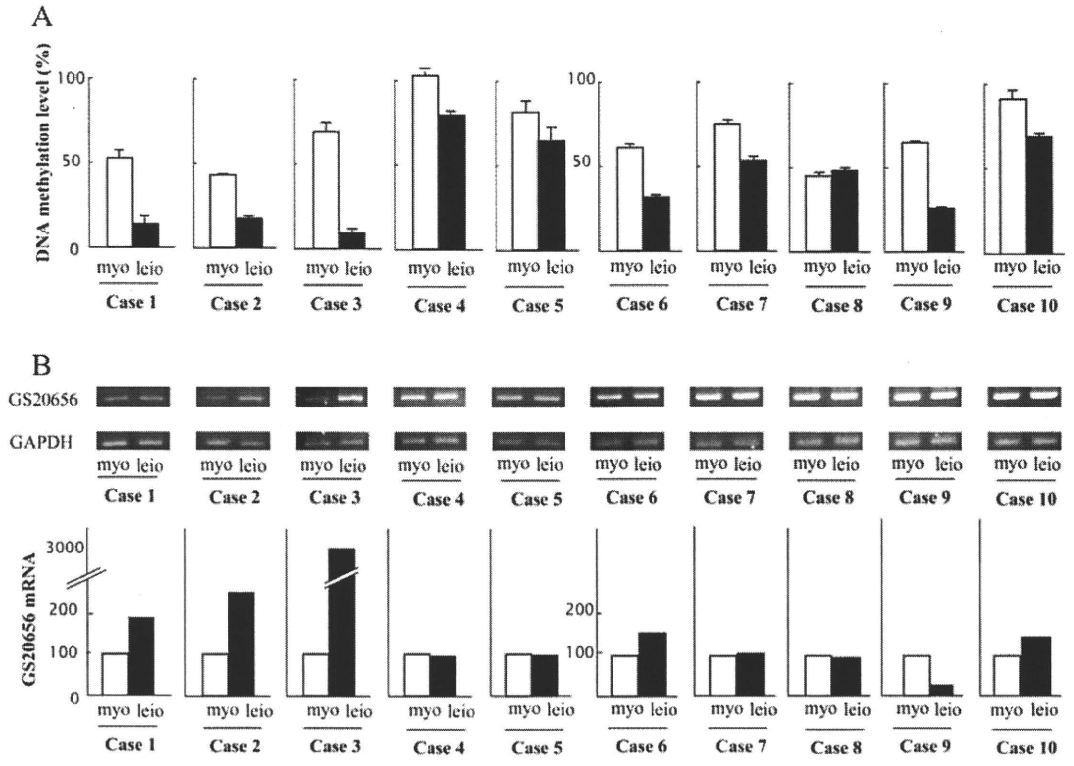

Figure 4 DNA methylation levels of the first exon of GS20656 and mRNA levels of GS20656. Methylation status of the first exon of GS20656 and mRNA expression of GS20656 were examined for 10 paired samples with leiomyoma (leio) and myometrium (myo). (**A**) DNA methylation levels were evaluated by methylation-sensitive quantitative real-time PCR, and expressed as %methylated DNA. Values are mean ± SD from three different experiments. Methylation levels were significantly different ($P < 0.05$, Student's *t*-test) between myometrium and leiomyoma in all cases except Case 8. (**B**) Representative blotting band of GS20656 and GAPDH by RT–PCR using primer set II, and mRNA expression of GS20656 by real-time RT–PCR using primer set I. Locations of primer sets I and II are shown in Fig. 1. Expression levels in the myometrium were normalized to 100% in each sample.

significant (Table III). There was no correlation between GS20656 mRNA expression and DNMT3b mRNA expression.

Discussion

The present study showed that uterine leiomyoma is associated with alterations of DNA methylation at multiple genomic loci as indicated by a genome-wide DNA methylation analysis using RLGS. The methylation status of 29 NotI sites was altered in uterine leiomyomas in comparison with normal myometrium. Intriguingly, both methylated and demethylated changes occurred at multiple gene loci in uterine leiomyomas. However, since there is a possibility that DNA methylation patterns differ among individuals, further RLGS analyses with larger samples are needed to clarify the detailed difference in genome-wide DNA methylation status between uterine leiomyomas and normal myometrium.

In this study, we identified a new putative gene, GS20656, which showed an aberrant methylation status in uterine leiomyomas compared with myometrium. The fact that the DNA methylation levels of the promoter region and the first exon of GS20656 were significantly lower in leiomyoma than in the myometrium indicates that GS20656 is regulated by DNA methylation in uterine leiomyomas. These results suggest that there is a gene under epigenetic regulation in uterine leiomyomas.

In the nine cases in which DNA methylation levels of GS20656 were lower in leiomyoma than in myometrium, five cases showed that GS20656 mRNA expression tended to be higher in leiomyoma than in myometrium. In particular, GS20656 mRNA expression is much higher in the cases that have considerable hypomethylation of GS20656 (Cases 1, 2 and 3 in Fig. 4). These results suggest that CpG sites of GS20656 may be associated with mRNA expression level of GS20656. However, it is not surprising that there are cases in which DNA methylation status of GS20656 is not consistent with GS20656 mRNA expression, because DNA methylation may occur heterogeneously and/or gradually and the change in DNA methylation varies among individuals. Our recent report also shows that there are cases in which DNA methylation status of ER-α promoter region is not consistent with ER-α mRNA expression (Asada *et al.*, 2008).

It would be interesting to know the biological role of GS20656. Although the participation of GS20656 in uterine leiomyomas may

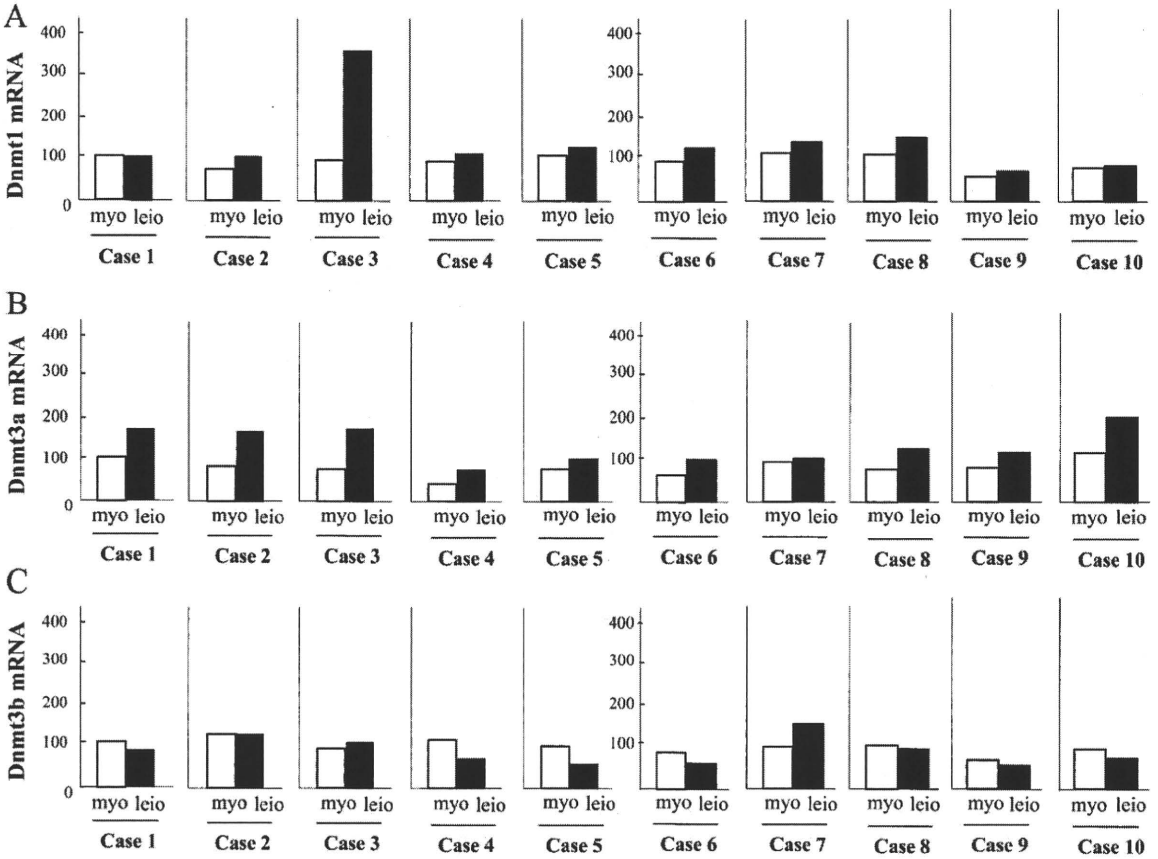

Figure 5 mRNA expression of DNMT in uterine leiomyoma (leio) and myometrium (myo). mRNA levels of DNMT1 (**A**), DNMT3a (**B**) and DNMT3b (**C**) were analyzed by real-time RT–PCR on the same 10 paired samples as shown in Fig. 4.

Table III DNMT mRNA levels in myometrium and leiomyoma

	n	Myometrium	Leiomyoma	Number of myo < leio
DNMT1	20	92.6 ± 5.0	118.6 ± 14.2[b]	15 (75%)
DNMT3a	20	110.5 ± 12.5	161.9 ± 19.8[a]	17 (85%)
DNMT3b	20	115.2 ± 8.6	97.2 ± 6.9	6 (30%)

mRNA levels of DNMT1, DNMT3a and DNMT3b were examined for 20 paired samples with leiomyoma (leio) and myometrium (myo) (Cases 1–20 in Table I). Values are mean ± SEM.
[a]$P < 0.01$ versus myometrium.
[b]$P < 0.05$ versus myometrium.

be different among the patients, further studies on the biological role of GS20656, including the relationship between GS20656 and clinical features such as tumor growth, phenotypes, hormone-responsiveness, etc, are needed.

Alterations in regional methylation patterns have been associated with silencing of tumor suppressor/DNA repair genes (Ballestar and Esteller, 2002), transcriptional activation of oncogenes (Feinberg *et al.*, 2002) and loss of imprinting in malignant cells (El-Osta, 2004), suggesting that hypermethylation is involved in the pathogenesis of malignant tumors. It is unclear that hypermethylation or hypomethylation is more important in the pathogenesis of uterine leiomyoma, which is a benign tumor. There are many differences in cell characteristics between malignant tumors and benign ones. Our RLGS analysis showed both methylated and demethylated changes in benign leiomyoma. Cell characteristics of uterine leiomyomas include the potential activities of both methylation and demethylation. This may be supported by the report of Li *et al.* (2003) that imbalanced methylation status, e.g. coexistence of global hypomethylation and local gene-specific hypermethylation, may exist in leiomyoma. The present result raises the possibility that epigenetic modification of DNA may be involved in the pathogenesis of uterine leiomyomas.

It is of interest that DNA methylation levels of normal myometrium vary among individuals. We previously reported that the DNA methylation status of the ER-α promoter region in normal myometrium varies among individuals, which may represent a physiological change in a certain cell type such as smooth muscle cells in myometrium (Asada *et al.*, 2008). Those results suggest that DNA

methylation seen in the myometrium may be caused by some factors that induce aberrant DNA methylation such as aging, chronic inflammation and possible viral infection (Ushijima and Okochi-Tanaka, 2005).

Li *et al.* (2003) showed that mRNA expression of DNMT3a and DNMT3b was lower in leiomyomas than in myometrium while most of the leiomyomas had equal or increased expression of DNMT1 compared with the myometrium. The present study showed mRNA levels of DNMT1 and DNMT3a were higher in leiomyomas than in myometrium, whereas there was no significant difference in DNMT3b mRNA expression between leiomyomas and myometrium. An increased DNMT1 expression was consistent in both studies, which may reflect an elevated proliferative activity of leiomyoma cells because DNMT1 is responsible for copying methylation patterns following DNA synthesis (Liu *et al.*, 1998). However, there was a discrepancy in DNMT3a and DNMT3b expression between the report by Li *et al.* (2003) and the present result. It is hard to clearly explain the inconsistency. This may be attributed to the race-dependent difference. The samples used in the report by Li *et al.* (2003) were obtained from 16 African-American, 5 Caucasian and 2 Hispanic women, whereas all samples in this study were from Japanese (Asian origin). In fact, it has recently been reported that the promoter which regulates aromatase expression in uterine leiomyomas is different between Japanese women and other race including African-American, Caucasian and Hispanic women (Shozu *et al.*, 2002; Imir *et al.*, 2007). In addition, it is well known that uterine fibroids are more common in African-American women than in white women (Faerstein *et al.*, 2001a, b). However, the findings from Li *et al.* (2003) and the present study both suggest the possibility that unusual expression of epigenetic factors causes aberrant DNA methylation in uterine leiomyomas.

Hattori *et al.* (2004a) showed DNA hypomethylation at genomic loci in Dnmt1$^{-/-}$ and Dnmt3a$^{-/-}$Dnmt3b$^{-/-}$ mouse ES cells compared with wild-type ES cells using an RLGS analysis. Furthermore, Ikegami *et al.* (2007) showed that G9a deficiency, which impairs histone H3-k9 methylation, caused DNA hypomethylation at the G9a target loci in G9a$^{-/-}$ mouse ES cells using RLGS. This indicates that global regulators could contribute to local changes in DNA methylation at genomic loci. It also implies that a combination of epigenetic factors is involved in the maintenance of DNA methylation in cells and tissues. It is apparent from our findings and other reports, further studies are needed regarding the relevance of epigenetic factors to the DNA methylation pattern in uterine leiomyomas.

In conclusion, the present study showed not only aberrant genome-wide DNA methylation status in uterine leiomyomas using RLGS but also the existence of a genomic locus that is differently methylated in normal myometrium and uterine leiomyoma. Epigenetics and DNA methylation-dependent gene regulation may play a role in formation and development of uterine leiomyomas.

Funding

This work was supported in part by Grants-in-Aid 17791121, 18791158, 19791153 and 20591918 for Scientific Research, and Program for Promotion of Basic Research Activities for Innovative Biosciences, from the Ministry of Education, Science, and Culture, Japan.

References

Ahn WS, Kim KW, Bae SM, Yoon JH, Lee JM, Namkoong SE, Kim JH, Kim CK, Lee YJ, Kim YW. Targeted cellular process profiling approach for uterine leiomyoma using cDNA microarray, proteomics and gene ontology analysis. *Int J Exp Pathol* 2003;**84**:267–279.

Asada H, Yamagata Y, Taketani T, Matsuoka A, Tamura H, Hattori N, Ohgane J, Hattori N, Shiota K, Sugino N. Potential link between estrogen receptor-α gene hypomethylation and uterine fibroid formation. *Mol Hum Reprod* 2008;**14**:539–545.

Ballestar E, Esteller M. The impact of chromatin in human cancer: linking DNA methylation to gene silencing. *Carcinogenesis* 2002;**23**:1103–1109.

Catherino WH, Leppert PC, Stenmark MH, Payson M, Potlog-Nahari C, Nieman LK, Segars JH. Reduced dermatopontin expression is a molecular link between uterine leiomyomas and keloids. *Genes Chromosomes Cancer* 2004;**40**:204–217.

Chiaffarino F, Parazzini F, La Vecchia C, Chatenoud L, Di Cintio E, Marsico S. Diet and uterine myomas. *Obstet Gynecol* 1999;**94**:395–398.

Cho J-H, Kimura H, Minami T, Ohgane J, Hattori N, Tanaka S, Shiota K. DNA methylation regulates placental lactogen I gene expression. *Endocrinology* 2001;**142**:3389–3396.

El-Osta A. The rise and fall of genomic methylation in cancer. *Leukemia* 2004;**18**:233–237.

Faerstein E, Szklo M, Rosenshein N. Risk factors for uterine leiomyoma: a practice-based case–control study I. African-American heritage, reproductive history, body size, and smoking. *Am J Epidemiol* 2001a; **153**:1–10.

Faerstein E, Szklo M, Rosenshein NB. Risk factors for uterine leiomyoma: a practice-based case–control study II. Atherogenic risk factors and potential sources of uterine irritation. *Am J Epidemiol* 2001b;**153**:11–19.

Feinberg AP, Cui H, Ohlsson R. DNA methylation and genomic imprinting: insights from cancer into epigenetic mechanisms. *Semin Cancer Biol* 2002;**12**:389–398.

Girault I, Tozlu S, Lidereau R, Bieche I. Expression analysis of DNA methyltransferases 1, 3A, and 3B in sporadic breast carcinomas. *Clin Cancer Res* 2003;**9**:4415–4422.

Hattori N, Abe T, Hattori N, Suzuki M, Matsuyama T, Yoshida S, Li E, Shiota K. Preference of DNA methyltransferases for CpG islands in mouse embryonic stem cells. *Genome Res* 2004a;**14**:1733–1740.

Hattori N, Nishino K, Ko YG, Hattori N, Ohgane J, Tanaka S, Shiota K. Epigenetic control of mouse Oct-4 gene expression in embryonic stem cells and trophoblast stem cells. *J Biol Chem* 2004b;**279**:17063–17069.

Heid CA, Stevens J, Livak KJ, Williams PM. Real time quantitative PCR. *Genome Res* 1996;**6**:986–994.

Hsieh CL. *In vivo* activity of murine *de novo* methyltransferases, Dnmt3a and Dnmt3b. *Mol Cell Biol* 1999;**19**:8211–8218.

Ikegami K, Iwatani M, Suzuki M, Tachibana M, Shinkai Y, Tanaka S, Greally JM, Yagi S, Hattori N, Shiota K. Genome-wide and locus-specific DNA hypomethylation in G9a deficient mouse embryonic stem cells. *Genes Cells* 2007;**12**:1–11.

Imamura T, Ohgane J, Ito S, Ogawa T, Hattori N, Tanaka S, Shiota K. CpG island of rat sphingosine kinase-1 gene: tissue-dependent DNA methylation status and multiple alternative first exons. *Genomics* 2001; **76**:117–125.

Imir AG, Lin Z, Yin P, Deb S, Yilmaz B, Cetin M, Cetin A, Bulun SE. Aromatase expression in uterine leiomyomata is regulated primarily by proximal promoters I.3/II. *J Clin Endocrinol Metab* 2007; **92**:1979–1982.

Kremenskoy M, Kremenska Y, Ohgane J, Hattori N, Tanaka S, Hashizume K, Shiota K. Genome-wide analysis of DNA methylation status of CpG islands in embryoid bodies, teratomas, and fetuses. *Biochem Biophys Res Commun* 2003;**311**:884–890.

Li E. Chromatin modification and epigenetic reprogramming in mammalian development. *Nat Rev Genet* 2002;**3**:662–673.

Li S, Chiang TC, Richard-Davis G, Barrett JC, McLachlan JA. DNA hypomethylation and imbalanced expression of DNA methyltransferases (DNMT1, 3A, and 3B) in human uterine leiomyoma. *Gynecol Oncol* 2003;**90**:123–130.

Liu Y, Okakeley EJ, Sun L, Jost JP. Multiple domains are involved in the targeting of the mouse DNA methyltransferase to the DNA replication foci. *Nucleic Acids Res* 1998;**26**:1038–1045.

Matsuyama T, Kimura MT, Koike K, Abe T, Nakano T, Asami T, Ebisuzaki T, Held WA, Yoshida S, Nagase H. Global methylation screening in the *Arabidopsis thaliana* and *Mus musculus* genome: applications of virtual image restriction landmark genomic scanning (Vi-RLGS). *Nucleic Acids Res* 2003;**31**:4490–4496.

Ryan GL, Syrop CH, Van Voorhis BJ. Role, epidemiology, and natural history of benign uterine mass lesions. *Clin Obstet Gynecol* 2005; **48**:312–324.

Shiota K. DNA methylation profiles of CpG islands for cellular differentiation and development in mammals. *Cytogenet Genome Res* 2004;**105**:325–334.

Shiota K, Yanagimachi R. Epigenetics by DNA methylation for development of normal and cloned animals. *Differentiation* 2002; **69**:162–166.

Shiota K, Kogo Y, Ohgane J, Imamura T, Urano A, Nishino K, Tanaka S, Hattori N. Epigenetic marks by DNA methylation specific to stem, germ and somatic cells in mice. *Genes Cells* 2002;**7**:961–969.

Shozu M, Sumitani H, Segawa T, Yang HJ, Murakami K, Kasai T, Inoue M. Overexpression of aromatase P450 in leiomyoma tissue is driven primarily through promoter I.4 of the aromatase P450 gene (CYP19). *J Clin Endocrinol Metab* 2002;**87**:2540–2548.

Smith SS. Biological implications of the mechanism of action of human DNA (cytosine-5)methyltransferase. *Prog Nucleic Acid Res Mol Biol* 1994;**49**:65–111.

Ting AH, Jair KW, Suzuki H, Yen RW, Baylin SB, Schuebel KE. Mammalian DNA methyltransferase 1: inspiration for new directions. *Cell Cycle* 2004;**3**:1024–1026.

Tsibris JC, Segars J, Coppola D, Mane S, Wilbanks GD, O'Brien WF, Spellacy WN. Insights from gene arrays on the development and growth regulation of uterine leiomyomata. *Fertil Steril* 2002;**78**:114–121.

Ushijima T, Okochi-Tanaka E. Aberrant methylations in cancer cells: where do they come from? *Cancer Sci* 2005;**96**:206–211.

Vollenhoven BJ, Lawrence AS, Healy DL. Uterine fibroids: a clinical review. *Br J Obstet Gyneacol* 1990;**97**:285–298.

Wang H, Mahadevappa M, Yamamoto K, Wen Y, Chen B, Warrington JA, Polan ML. Distinctive proliferative phase differences in gene expression in human myometrium and leiomyomata. *Fertil Steril* 2003;**80**:266–276.

Weston G, Trajstman AC, Gargett CE, Manuelpillai U, Vollenhoven BJ, Rogers PA. Fibroids display an anti-angiogenic gene expression profile when compared with adjacent myometrium. *Mol Hum Reprod* 2003; **9**:541–549.

Submitted on November 2, 2008; resubmitted on December 19, 2008; accepted on January 29, 2009

Human Reproduction, Vol.24, No.5 pp. 1126–1132, 2009
Advanced Access publication on February 6, 2009 doi:10.1093/humrep/dep015

human reproduction **ORIGINAL ARTICLE** *Reproductive biology*

DNA methyltransferase expression in the human endometrium: down-regulation by progesterone and estrogen

Yoshiaki Yamagata, Hiromi Asada, Isao Tamura, Lifa Lee, Ryo Maekawa, Ken Taniguchi, Toshiaki Taketani, Aki Matsuoka, Hiroshi Tamura, and Norihiro Sugino[1]

Department of Obstetrics and Gynecology, Yamaguchi University Graduate School of Medicine, Minamikogushi 1-1-1, Ube 755-8505, Japan

[1]Correspondence address. Tel: +81-836-22-2286; Fax: +81 836-22-2287; E-mail: sugino@yamaguchi-u.ac.jp

BACKGROUND: Epigenetic regulation may be involved in modulation of gene expression during the normal cyclic changes of the human endometrium. We investigated expression of DNA methyltransferases (DNMTs) in endometrium during the menstrual cycle and the influence of sex steroid hormones on DNMT in endometrial stromal cells (ESC) in culture.

METHODS: Expression of DNMT1, DNMT3a and DNMT3b was assessed by immunohistochemistry and real-time RT–PCR in endometrial tissue ($n = 42$ women). ESC ($n = 3$ women) were cultured with estradiol and medroxyprogesterone acetate (E + MPA) for 17 days, and DNMT mRNA levels were measured by real-time RT–PCR.

RESULTS: Nuclei of both epithelial and stromal cells immunostained for DNMT1, DNMT3a and DNMT3b during each phase of the menstrual cycle. Tissue levels of DNMT1 and DNMT3a mRNA were significantly lower in the mid-secretory phase than in the proliferative phase ($P < 0.01$). For DNMT3b, the change in mRNA levels showed a similar trend to that for DNMT3a. In ESC culture, DNMT3a and DNMT3b mRNA levels were significantly decreased by E + MPA treatment ($P < 0.01$ and $P < 0.05$, respectively) at Day 8 and Day 17.

CONCLUSIONS: DNMT mRNAs declined in the human endometrium during the secretory phase, and E + MPA down-regulated DNMT3a and DNMT3b mRNAs in ESC in culture. These results suggest that DNMTs have regulatory functions in gene expression that is associated with decidualization.

Key words: DNA methyltransferase / endometrium / endometrial stromal cell / decidualization

Introduction

The human endometrium, which mainly consists of endometrial epithelial cells and endometrial stromal cells (ESC), has cyclic changes in morphology and in function depending on female sex steroid hormone exposure. These cells actively proliferate under estrogen exposure during the proliferative phase and thereafter differentiate under progesterone exposure during the secretory phase. A number of genes are involved in proliferation, differentiation and tissue breakdown in the endometrium under the influence of female sex steroid hormones (Sugino *et al.*, 2002a, 2004; Ace and Okulicz, 2004; Ponnampalam *et al.*, 2004). A great number of genes are up-regulated or down-regulated in the human endometrium during decidualization, which occurs around the time of embryo implantation (Popovici *et al.*, 2000; Kao *et al.*, 2002; Okada *et al.*, 2003; Riesewijk *et al.*, 2003; Ace and Okulicz, 2004; Mirkin *et al.*, 2005), suggesting the presence of complex mechanisms of gene expression. However, little is known about the molecular mechanisms involved in the regulation of gene expression in the human endometrium.

In the last decades, it has become clear that epigenetic regulation, including DNA methylation and histone modification, plays a key role in transcriptional regulation. DNA methylation occurs at cytosines within CpG dinucleotides that are clustered frequently in regions of ~1–2 kb in length, called CpG islands, in or near the promoter and first exon regions of genes (Esteller *et al.*, 2002; Jones and Baylin, 2002). DNA methylation at the CpG dinucleotides is a post-replication event catalyzed by DNA methyltransferase (DNMT) (Smith, 1994) that adds a methyl group to the cytosine ring to form

© The Author 2009. Published by Oxford University Press on behalf of the European Society of Human Reproduction and Embryology. All rights reserved.
For Permissions, please email: journals.permissions@oxfordjournals.org

methyl cytosine, which establishes normal methylation patterns during embryogenesis and reproduces these patterns during replication of adult cells (Li *et al.*, 1993; Razin and Kafri, 1994). DNA methylation is an important mechanism of epigenetic gene regulation, and is involved in genomic imprinting, X chromosomal inactivation, aging, mutagenesis and regulation of tissue-specific gene expression during development and adult life (Li *et al.*, 1993; Razin and Kafri, 1994; Ohgane *et al.*, 1998; Imamura *et al.*, 2001; Li, 2002; Shiota and Yanagimachi, 2002). Aberrant methylation of CpG islands, located in the 5′-promoter region of genes, is commonly associated with transcriptional inactivation (Nan *et al.*, 1998). Such inactivation is well known in various human cancers, especially in tumor suppressor genes (Ushijima and Okochi-Takada, 2005).

Several DNMTs exist. DNMT1 functions as a 'maintenance' DNMT in mammalian cells and is therefore responsible for accurately replicating genomic DNA methylation patterns during cell division (Liu *et al.*, 1998). On the other hand, DNMT3a and DNMT3b are thought to catalyze *de novo* methylation of DNA (Hsieh, 1999). Recent research also shows that DNMT1, DNMT3a and DNMT3b co-operatively maintain DNA methylation (Ting *et al.*, 2004).

Recently, aberrant expression of DNMTs was observed in endometriosis, which is a non-cancerous ectopic growth of the human endometrium (Wu *et al.*, 2007). Aberrant DNA methylation of the promoter region is involved in aberrant gene expression of steroidogenic factor-1 and estrogen receptor in endometriosis (Xue *et al.*, 2007a, b; Utsunomiya *et al.*, 2008). Furthermore, in the eutopic endometrium of women with endometriosis, reduced expression of HOXA10, which is a transcription factor and plays an important role in uterine receptivity, was found to be due to DNA methylation of the promoter region (Wu *et al.*, 2005). In addition, aromatase expression in ESC is under epigenetic regulation (Izawa *et al.*, 2008). Histone acetylation is involved in differentiation of ESC and endometrial epithelial cells (Sakai *et al.*, 2003; Uchida *et al.*, 2005). These reports led us to hypothesize that epigenetic regulation is involved in the normal cyclic changes of the human endometrium. To test this hypothesis, we investigated changes in the expression of DNMTs in the normal endometrium during the menstrual cycle and the influence of female sex steroid hormones on DNMT expression in ESC.

Materials and Methods

This study was reviewed and approved by the Institutional Review Board of Yamaguchi University Graduate School of Medicine. Informed consent was obtained from the women before collection of any samples for this study.

Tissue samples

Endometrial tissues were collected from hysterectomy specimens or biopsies for histological dating of the endometrium in 42 women with regular menstrual cycles (aged 22–50 years, median 36.9 years). All of the women received no steroid medications. Endometria were dated according to the histological criteria by Noyes *et al.* (1950) and were classified into four different groups: proliferative phase (days 6–14, $n = 14$), early secretory phase (days 15–18, $n = 10$), mid-secretory phase (days 19–23, $n = 11$) and late secretory phase (days 24–28, $n = 7$). Endometrial samples were snap-frozen in liquid nitrogen and stored at −80°C until RNA isolation. For immunohistochemistry, the tissue specimens were fixed in 10% buffered formalin and embedded in paraffin.

Immunohistochemistry

Immunohistochemistry for DNMTs in the endometrium was performed on 4 μm thick paraffin sections mounted on silane-coated glass slides (Dako, Glostrup, Denmark) using anti-DNMT1 monoclonal antibody (IMG-261 mouse; Imgenex, San Diego, CA, USA), anti-DNMT3a polyclonal antibody (RB1852 rabbit; Abgent, San Diego, CA, USA) or anti-DNMT3b polyclonal antibody (RB1906 rabbit; Imgenex), as reported previously (Sugino *et al.*, 1996, 2002b). Briefly, the sections were deparaffinized in xylene and dehydrated through a graded series of ethanol. For antigen retrieval, the sections were autoclaved at 121°C for 15 min. Endogenous peroxidase activities and non-specific binding were then blocked with 1% H_2O_2 and 10% normal rabbit serum (Nichirei, Tokyo, Japan) for DNMT1 or 10% normal goat serum (Nichirei) for DNMT3a and DNMT3b, respectively. The sections were then incubated with the primary antibody diluted 1:50 overnight at 4°C. Parallel control sections were incubated with normal mouse serum or normal rabbit serum (Dako) instead of specific primary antibodies. Biotinylated antimouse antibody (Nichirei) for DNMT1 or biotinylated antirabbit antibody (Nichirei) for DNMT3a and DNMT3b was used as the secondary antibody. After the sections were rinsed in phosphate-buffered saline (PBS), they were incubated in streptavidin–peroxidase complex (Nichirei) for 5 min, rinsed in PBS and then visualized with diaminobenzidine and counterstained with hematoxylin. Dark brown nuclear staining indicated a positive reaction. The histological sections were independently evaluated by three observers, and relative intensities of the signals were estimated at + (weakly positive) to +++ (strongly positive).

ESC culture

For ESC culture, endometrial tissues that were histologically diagnosed as being in the late proliferative phase were used. Tissue samples were obtained from three individuals, and cells from an individual were cultured in triplicate. ESC were isolated as reported previously (Sugino *et al.*, 2000, 2002c). Endometrial tissues were washed with phenol red-free Dulbecco's modified Eagle's medium (DMEM) (Invitrogen, Paisley, UK) containing 4 mmol/l glutamine (Invitrogen), 50 μg/ml streptomycin (Invitrogen) and 50 IU/ml penicillin (Invitrogen), and minced into small pieces of <1 mm^3. After the enzymatic digestion of minced tissues with 0.2% collagenase (Sigma, St Louis, MO, USA) in a shaking water bath for 2 h at 37°C, ESC were separated by filtration through a 70 μm nylon mesh. The filtrates were washed three times, and the number of viable cells was counted by trypan blue dye exclusion. The homogeneity of the stromal cell preparation (98%) was verified by immunocytochemistry using an antibody against vimentin, a specific marker of stromal cells. ESC were seeded at 10^5 cells/cm^2 in 75 cm^2 tissue culture flasks and grown until confluence in phenol red-free DMEM containing glutamine, antibiotics and 10% dextran-coated charcoal-stripped fetal calf serum (FCS) (Biological Industries, Kibbutz Beit Haemek, Israel) at 37°C, 95% air and 5% CO_2. If necessary, cells were subcultured in 75 cm^2 tissue culture flasks after the first passage until confluence. For treatments, cells were subcultured into 25 cm^2 tissue culture flasks (second or third passage), and the cell culture medium was changed to the treatment medium at 80% confluence.

To examine the effect of estrogen and progesterone on DNMTs mRNA levels in ESC, cells were incubated with treatment medium (phenol red-free DMEM supplemented with glutamine, antibiotics and 2% stripped FCS) containing a combination of estradiol (10^{-8} M) (Sigma) and medroxyprogesterone acetate (MPA, 10^{-6} M) (Sigma) for 17 days at 37°C, in 95% air and 5% CO_2. The concentrations of estradiol and MPA, and the period of incubation were based on our previous reports (Sugino *et al.*, 2000, 2002d). The medium was changed every other day. Decidualization was

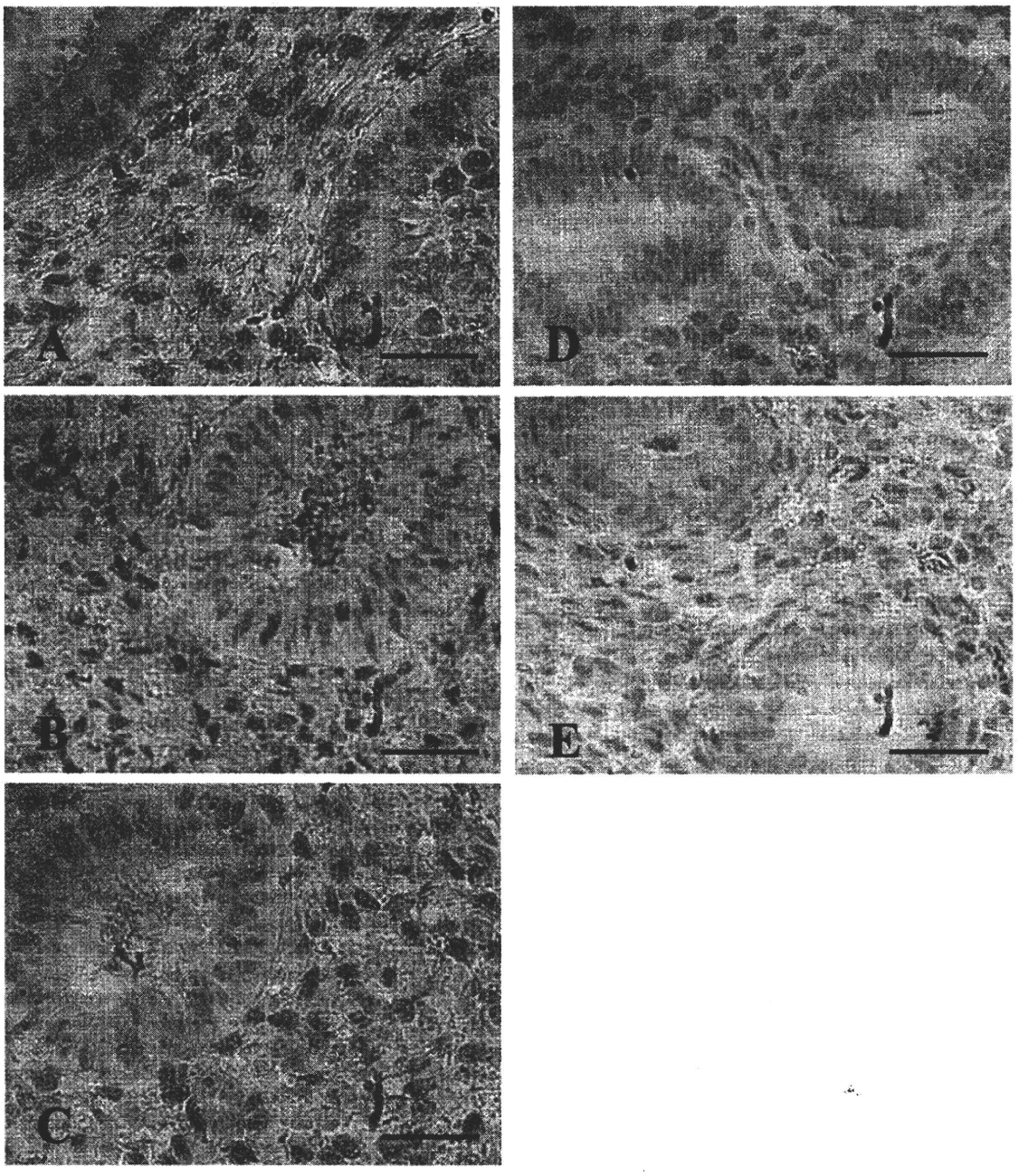

Figure 1 Immunohistochemical staining for DNMT1, DNMT3a and DNMT3b in the human endometrium. Immunohistochemical staining was performed on tissue samples from the proliferative phase, early secretory phase, mid-secretory phase and late secretory phase. Tissue samples were taken from three different patients in each phase. Representative results from the late proliferative phase are shown. Nuclei of both epithelial cells and stromal cells immunostained for DNMT1 (**A**), DNMT3a (**B**) and DNMT3b (**C**). No immunoreactivity was observed in the control sections incubated with normal mouse serum (**D**) and normal rabbit serum (**E**). Bar = 50 μm.

confirmed by morphology and mRNA expression of insulin-like growth factor-binding protein-1 (IGFBP-1), which is a specific marker of decidualization (Giudice *et al.*, 1992; Sugino *et al.*, 2000). Total RNA was isolated from cultured cells, and RT–PCR for DNMTs was performed as described below, with a duplicate PCR for each culture.

Real-time RT–PCR

Total RNA was extracted from endometrial tissues and cultured cells us Isogen (Wako, Osaka, Japan), and real-time RT–PCR was performed reported previously (Asada *et al.*, 2008). RT reactions were perform with ExScript RT reagent kit (TAKARA, Kyoto, Japan) according to

manufacturer's protocol. Briefly, 2 μg of total RNA was incubated with 4 μl of 5× ExCript buffer, 1 μl of dNTP mixture (10 mM each), 1 μl of Random primers (50 μM), 0.5 μl of ExCript reverse transcriptase (200 U/μl) and 0.5 μl of RNase inhibitor (40 U/μl) in 20 μl of reaction mixture at 42°C for 15 min, after which the reverse transcriptase was inactivated by heating the samples at 95°C for 2 min. The complementary DNA (cDNA) was immediately used for PCR. All PCRs were performed using SYBR Premix Ex Taq (TAKARA) and a LightCycler (Roche Applied Science, Basel, Switzerland). Briefly, 2 μl of aliquots containing cDNA were amplified in a total volume of 20 μl containing 4 μl of a 5× SYBR PreMix Ex Taq and 0.2 μM each primer. For internal controls, TATA box-binding protein (TBP) cDNA or glyceraldehyde-3-phosphate dehydrogenase (GAPDH) was also amplified. According to the previous report (Girault *et al.*, 2003), the following primers were used: DNMT1 (forward, 5′-TACCTGGACGACCCTGACCTC-3′, reverse, 5′-CGTTGG CATCAAAGATGGACA-3′) (product size: 103 bp); DNMT3a (forward, 5′-TATTGATGAGCGCACAAGAGAGC-3′, reverse, 5′-GGGTGTTCCA GGGTAACATTGAG-3′) (111 bp); DNMT3b (forward, 5′-GGCAAG TTCTCCGAGGTCTCTG-3′, reverse, 5′-TGGTACATGGCTTTTCGA TAGGA-3′) (113 bp); TBP (forward, 5′-TGCACAGGAGCCAAGAGTG AA-3′, reverse, 5′-CACATCACAGCTCCCCACCA-3′) (132 bp); IG FBP-1 (forward, 5′-CGAAGGCTCTCCATGTCACCA-3′, reverse, 5′-TG TCTCCTGTGCCTTGGCTAAAC-3′) (98 bp) and GAPDH (forward, 5′-AGGTGAAGGTCGGAGTCA-3′, reverse, 5′-GGTCATTGATGG CAACAA-3′) (99 bp). All samples were run in duplicate. For appropriate negative controls, the RNA template was replaced with nuclease-free water in each run. Melting curves of the products were obtained after cycling by a stepwise increase of temperature from 55 to 95°C. At the end of 40 cycles, reaction products were separated electrophoretically on an agarose gel and stained with ethidium bromide for visual confirmation of the PCR products.

Statistical analyses

Statistical analysis was carried out using the Statistical Package for the Social Sciences for windows 13.0. To evaluate whether tissue mRNA levels significantly vary during the menstrual cycle, the Tukey honest significant difference test was used. For ESC cultures, differences in mRNA levels were determined using Duncan's new multiple range test. $P < 0.05$ was considered to be significant.

Results

Nuclei of both epithelial cells and stromal cells in tissue sections immunostained for DNMT1, DNMT3a and DNMT3b during each phase of the menstrual cycle. Representative results from the late proliferative phase are shown in Fig. 1. The staining intensities did not vary among the menstrual phases.

Changes in DNMT1, DNMT3a and DNMT3b mRNA levels in the endometrial tissue are shown in Fig. 2. DNMT1 mRNA levels were significantly lower in the mid-secretory phase than in the other menstrual phases (Fig. 2A). DNMT3a mRNA levels were significantly lower in the secretory phase than in the proliferative phase (Fig. 2B), being lowest in the mid-secretory phase (Fig. 2B). The pattern of change in the DNMT3b mRNA levels was similar to that for DNMT3a, but the changes were not statistically significant (Fig. 2C).

Since mRNA levels of DNMT1, DNMT3a and DNMT3b in the endometrium were lower in the mid-secretory phase than in the proliferative phase, we examined whether DNMT mRNA expression is influenced by progesterone and estrogen. We therefore focused on

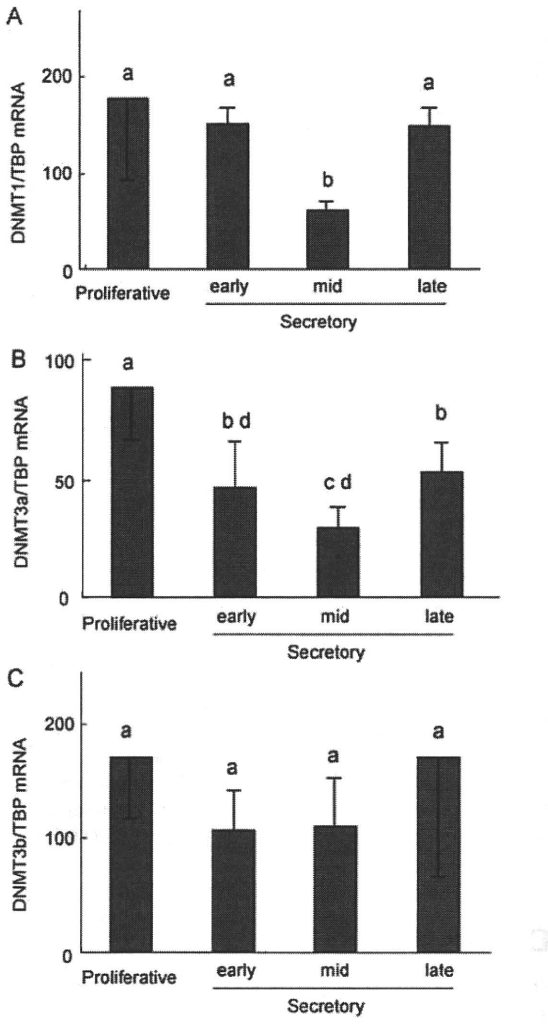

Figure 2 Changes in mRNA levels of DNMT1 (**A**), DNMT3a (**B**) and DNMT3b (**C**) in the human endometrium during the menstrual cycle. Total RNA was isolated from endometrial tissues and subjected to real-time RT–PCR. Endometrial tissues were obtained from the proliferative phase ($n = 14$), early secretory phase ($n = 10$), mid-secretory phase ($n = 11$) and late secretory phase ($n = 7$). Relative mRNA expression normalized to TBP (internal control) was calculated. Values are mean ± SD. Different letters indicate significant differences between groups ($P < 0.01$ in A, $P < 0.05$ in B).

ESC, which differentiate to decidualized stromal cells under the influence of progesterone and estrogen during the secretory phase. In order to induce decidualization *in vitro*, ESC were treated with MPA and estradiol for 17 days. As shown in Fig. 3A, mRNA expression of IGFBP-1, a specific marker of decidualization, was clearly induced by MPA and estradiol for 17 days. DNMT3a and DNMT3b mRNA levels were gradually decreased by MPA + estradiol and were significantly lower in the MPA + estradiol group than in the control group on days 8 and 17 after treatment (Fig. 3C and D). However, DNMT1 mRNA levels did not change during the treatment (Fig. 3B).

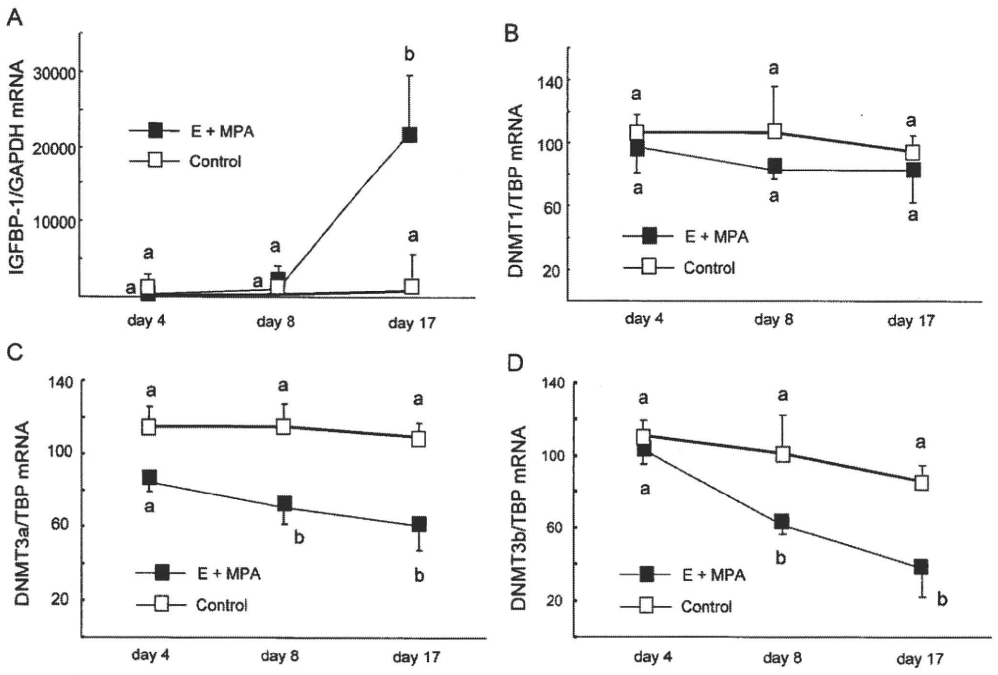

Figure 3 Effects of progesterone and estrogen on mRNA expression of DNMT1 (**B**), DNMT3a (**C**) and DNMT3b (**D**) in cultured ESC. Tissues were obtained from three individuals, and the cells from an individual were cultured in triplicate. Cells were treated with estradiol (E, 10^{-8} M) and MPA (10^{-6} M) for 17 days to induce decidualization *in vitro*. Decidualization was confirmed by mRNA expression of IGFBP-1, which is a specific marker of decidualization (**A**). Total RNA was isolated from cultured cells, and real-time RT–PCR for DNMTs or IGFBP-1 was performed and relative mRNA expression was calculated as described in Materials and Methods section. Values are mean ± SEM of three different cultures. Different letters indicate significant differences between groups ($P < 0.05$ in A and D, $P < 0.01$ in C).

Discussion

The present study showed changes in the level of DNMT mRNAs in the human endometrium during the menstrual cycle. DNMT3a mRNA levels were significantly lower in the secretory phase than in the proliferative phase, being lowest in the mid-secretory phase. The pattern of change in DNMT3b mRNA levels was similar to that for DNMT3a. Furthermore, we showed that DNMT3a and DNMT3b mRNA level in ESC was down-regulated by MPA and estrogen. DNMT3a and DNMT3b are responsible for *de novo* CpG methylation (Hsieh, 1999). CpG methylation of the promoter region inactivates gene expression (Nan *et al.*, 1998; Ushijima and Okochi-Takada, 2005). These findings lead us to speculate that the down-regulation of DNMT3a and DNMT3b mRNAs may be associated with expression of the genes that are induced during decidualization. In fact, a great number of genes are up-regulated and some genes are newly expressed in the human endometrium undergoing decidualization (Popovici *et al.*, 2000; Kao *et al.*, 2002; Riesewijk *et al.*, 2003; Ace and Okulicz, 2004; Mirkin *et al.*, 2005). Further studies are needed to find out which genes are regulated by DNA methylation during decidualization.

In the present study, DNMT1 mRNA levels in the endometrial tissue were significantly lower in the mid-secretory than in the proliferative phase, whereas DNMT1 mRNA levels were not affected by MPA and estradiol in ESC undergoing decidualization. Therefore, the low levels of DNMT1 in the mid-secretory phase endometrium may reflect the levels in the endometrial epithelium rather than the levels in the ESC. DNMT1 is responsible for accurately replicating genomic DNA methylation patterns to maintain genome stability during cell division (Liu *et al.*, 1998). Endometrial epithelial cells do not proliferate during the mid-secretory phase, which seems to be compatible with the decreased DNMT1 expression during the mid-secretory phase.

There seems to be a discrepancy in this study between mRNA and protein levels for DNMT, and this may be due to the different sensitivities of RT–PCR and immunohistochemistry.

Little information is available regarding the regulation of DNMT expression. Interestingly, the present study showed that DNMT3a and DNMT3b are under the regulation of female sex steroid hormones, suggesting that DNA methylation may be influenced by female sex steroid hormones. It has been reported that DNA methylation status can be altered by a variety of factors including steroids and vitamins (Shiota, 2004). On the other hand, DNA methylation affects estrogen receptors in endometria, mammary glands and myometrium (Lapidus *et al.*, 1996; Iwase *et al.*, 1999; Giacinti *et al.*, 2006; Asada *et al.*, 2008). These findings suggest a close relationship between DNA methylation and female sex steroid hormones. However, further study is needed to clarify the molecular mechanisms of regulation of DNMTs expression.

The phase-specific and transient changes in the DNMT mRNAs during the menstrual cycle may suggest that DNA methylation status is changeable during the menstrual cycle, which may lead to changes in transcription levels of some genes. This is supported by recent reports that DNMTs are involved in both methylation and demethylation of CpG dinucleotides in human cells with cyclical changes in DNA methylation status (Kangaspeska *et al.*, 2008; Metivier *et al.*, 2008).

This study showed that DNMT mRNA levels change in the human endometrium during the menstrual cycle and that DNMT3a and DNMT3b mRNAs in ESC can be regulated by female sex steroid hormones. These results suggest that DNMTs have regulatory functions on gene expression in the human endometrium. Further studies are needed to show a potential role of epigenetic regulation in gene expression that is associated with decidualization.

Authors contribution

Y.Y.: conception and design, acquisition of data, analysis of data and drafting the article; H.A., L.L., I.T., R.M., K.T., T.T., A.M. and H.T.: acquisition of data and N.S.: conception and design, interpretation of data, drafting the article and final approval.

Funding

This work was supported in part by Grants-in-Aid 17791121, 18791158, 19791153 and 20591918 for Scientific Research from the Ministry of Education, Science, and Culture, Japan.

References

Ace CI, Okulicz WC. Microarray profiling of progesterone-regulated endometrial genes during the rhesus monkey secretory phase. *Reprod Biol Endocrinol* 2004;**2**:54.

Asada H, Yamagata Y, Taketani T, Matsuoka A, Tamura H, Hattori N, Ohgane J, Hattori N, Shiota K, Sugino N. Potential link between estrogen receptor-α gene hypomethylation and uterine fibroid formation. *Mol Hum Reprod* 2008;**14**:539–545.

Esteller M, Fraga MF, Paz MF, Campo E, Colomer D, Novo FJ, Calasanz MJ, Galm O, Guo M, Benitez J *et al.* Cancer epigenetics and methylation. *Science* 2002;**297**:1807–1808.

Giacinti L, Claudio PP, Lopez M, Giordano A. Epigenetic information and estrogen receptor alpha expression in breast cancer. *Oncologist* 2006; **11**:1–8.

Girault I, Tozlu S, Lidereau R, Bieche I. Expression analysis of DNA methyltransferases 1, 3A, and 3B in sporadic breast carcinomas. *Clin Cancer Res* 2003;**9**:4415–4422.

Giudice LC, Dsupin BA, Irwin JC. Steroid and peptide regulation of insulin-like growth factor-binding proteins secreted by human endometrial stromal cells is dependent on stromal differentiation. *J Clin Endocrinol Metab* 1992;**75**:1235–1241.

Hsieh CL. *In vivo* activity of murine de novo methyltransferases, DNMT3a and DNMT3b. *Mol Cell Biol* 1999;**19**:8211–8218.

Imamura T, Ohgane J, Ito S, Ogawa T, Hattori N, Tanaka S, Shiota K. CpG island of rat sphingosine kinase-1 gene: tissue-dependent DNA methylation status and multiple alternative first exons. *Genomics* 2001; **76**:117–125.

Iwase H, Omoto Y, Iwata H, Toyama T, Hara Y, Ando Y, Ito Y, Fujii Y, Kobayashi S. DNA methylation analysis at distal and proximal promoter regions of the oestrogen receptor gene in breast cancer. *Br J Cancer* 1999;**80**:1982–1986.

Izawa M, Harada T, Taniguchi F, Ohama Y, Takenaka Y, Terakawa N. An epigenetic disorder may cause aberrant expression of aromatase gene in endometriotic stromal cells. *Fertil Steril* 2008;**89**:1390–1396.

Jones PA, Baylin SB. The fundamental role of epigenetic events in cancer. *Nature Rev* 2002;**3**:415–428.

Kangaspeska S, Stride B, Metivier R, Polycarpou-Schwarz M, Ibberson D, Carmouche RP, Benes V, Gannon F, Reid G. Transient cyclical methylation of promoter DNA. *Nature* 2008;**452**:112–115.

Kao LC, Tulac S, Lobo S, Imani B, Yang JP, Germeyer A, Osteen K, Taylor RN, Lessey BA, Giudice LC. Global gene profiling in human endometrium during the window of implantation. *Endocrinology* 2002; **143**:2119–2138.

Lapidus RG, Ferguson AT, Ottaviano YL, Parl FF, Smith HS, Weitzman SA, Baylin SB, Issa J-P, Davidson NE. Methylation of estrogen and progesterone receptor gene 5′ CpG islands correlates with lack of estrogen and progesterone receptor gene expression in breast tumors. *Clin Cancer Res* 1996;**2**:805–810.

Li E. Chromatin modification and epigenetic reprogramming in mammalian development. *Nat Rev Genet* 2002;**3**:662–673.

Li E, Beard C, Jaenisch R. Role for DNA methylation in genomic imprinting. *Nature* 1993;**366**:362–365.

Liu Y, Okakeley EJ, Sun L, Jost JP. Multiple domains are involved in the targeting of the mouse DNA methyltransferase to the DNA replication foci. *Nucleic Acids Res* 1998;**26**:1038–1045.

Metivier R, Gallais R, Tiffoche C, Le Peron C, Jurkowska RZ, Carmouche RP, Ibberson D, Barath P, Demay F, Reid G *et al.* Cyclical DNA methylation of a transcriptionally active promoter. *Nature* 2008; **452**:45–50.

Mirkin S, Arslan M, Churikov D, Corica A, Diaz JI, Williams S, Bocca S, Oehninger S. In search of candidate genes critically expressed in the human endometrium during the window of implantation. *Hum Reprod* 2005;**20**:2104–2117.

Nan X, Ng H-H, Johnson CA, Laherty CD, Turner BM, Eisenman RN, Bird A. Transcriptional repression by the methyl-CpG-binding protein MeCP2 involves a histone deacetylase complex. *Nature* 1998; **393**:386–389.

Noyes RW, Hertig AT, Rock J. Dating the endometrial biopsy. *Fertil Steril* 1950;**1**:3–25.

Ohgane J, Aikawa J, Ogura A, Hattori N, Ogawa T, Shiota K. Analysis of CpG islands of trophoblast giant cells by restriction landmark genomic scanning. *Dev Genet* 1998;**22**:132–140.

Okada H, Nakajima T, Yoshimura T, Yasuda K, Kanzaki H. Microarray analysis of genes controlled by progesterone in human endometrial stromal cells. *Gynecol Endocrinol* 2003;**17**:271–280.

Ponnampalam AP, Weston GC, Trajstman AC, Susil B, Rogers PAW. *Molecular classification of human endometrial cycle stages by* transcriptional profiling. *Mol Hum Reprod* 2004;**10**:879–893.

Popovici RM, Kao LC, Giudice LC. Discovery of new inducible genes in *in vitro* decidualized human endometrial stromal cells using microarray technology. *Endocrinology* 2000;**141**:3510–3513.

Razin A, Kafri T. DNA methylation from embryo to adult. *Prog Nucleic Acid Res Mol Biol* 1994;**48**:53–81.

Riesewijk A, Martin J, Os RV, Horcajadas JA, Polman J, Pellicer A, Mosselman S, Simon C. Gene expression profiling of human endometrial receptivity on days LH+2 versus LH+7 by microarray technology. *Mol Hum Reprod* 2003;**9**:253–264.

Sakai N, Maruyama T, Sakurai R, Masuda H, Yamamoto Y, Shimizu A, Kishi I, Asada H, Yamagoe S, Yoshimura Y. Involvement of histone acetylation in ovarian steroid-induced decidualization of human endometrial stromal cells. *J Biol Chem* 2003;**278**:16675–16682.

Shiota K. DNA methylation profiles of CpG islands for cellular differentiation and development in mammals. *Cytogenet Genome Res* 2004;**105**:325–334.

Shiota K, Yanagimachi R. Epigenetics by DNA methylation for development of normal and cloned animals. *Differentiation* 2002;**69**:162–166.

Smith SS. Biological implications of the mechanism of action of human DNA (cytosine-5)methyltransferase. *Prog Nucleic Acid Res Mol Biol* 1994;**49**:65–111.

Sugino N, Shimamura K, Takiguchi S, Tamura H, Ono M, Nakata M, Nakamura Y, Ogino K, Uda T, Kato H. Changes in activity of superoxide dismutase in the human endometrium throughout the menstrual cycle and in early pregnancy. *Hum Reprod* 1996;**11**:1073–1078.

Sugino N, Kashida S, Takiguchi S, Nakamura Y, Kato H. Induction of superoxide dismutase by decidualization in human endometrial stromal cells. *Mol Hum Reprod* 2000;**6**:178–184.

Sugino N, Karube-Harada A, Kashida S, Takiguchi S, Kato H. Differential regulation of copper-zinc superoxide dismutase and manganese superoxide dismutase by progesterone withdrawal in human endometrial stromal cells. *Mol Hum Reprod* 2002a;**8**:68–74.

Sugino N, Kashida S, Karube-Harada A, Takiguchi S, Kato H. Expression of vascular endothelial growth factor and its receptors in the human endometrium throughout the menstrual cycle and in early pregnancy. *Reproduction* 2002b;**123**:379–387.

Sugino N, Karube-Harada A, Sakata A, Takiguchi S, Kato H. Nuclear factor-κB is required for tumor necrosis factor-alpha induced manganese superoxide dismutase expression in human endometrial stromal cells. *J Clin Endocrinol Metab* 2002c;**87**:3845–3850.

Sugino N, Karube-Harada A, Sakata A, Takiguchi S, Kato H. Different mechanisms for the induction of copper-zinc superoxide dismutase and manganese superoxide dismutase by progesterone in human endometrial stromal cells. *Hum Reprod* 2002d;**17**:1709–1714.

Sugino N, Karube-Harada A, Taketani T, Sakata A, Nakamura Y. Withdrawal of ovarian steroids stimulates prostaglandin F2α production through nuclear factor-κB activation via oxygen radicals in human endometrial stromal cells: potential relevance to menstruation. *J Reprod Dev* 2004;**50**:215–225.

Ting AH, Jair KW, Suzuki H, Yen RW, Baylin SB, Schuebel KE. Mammalian DNA methyltransferase 1: inspiration for new directions. *Cell Cycle* 2004;**3**:1024–1026.

Uchida H, Maruyama T, Nagashima T, Asada H, Yoshimura Y. Histone deacetylase inhibitors induce differentiation of human endometrial adenocarcinoma cells through up-regulation of glycodelin. *Endocrinology* 2005;**146**:5365–5373.

Ushijima T, Okochi-Takada E. Aberrant methylations in cancer cells: where do they come from? *Cancer Sci* 2005;**96**:206–211.

Utsunomiya H, Cheng YH, Lin Z, Reierstad S, Yin P, Attar E, Xue Q, Imir G, Thung S, Trukhacheva E *et al.* Upstream stimulatory factor-2 regulates steroidogenic factor-1 expression in endometriosis. *Mol Endocrinol* 2008;**22**:904–914.

Wu Y, Halverson G, Basir Z, Strawn E, Yan P, Guo SW. Aberrant methylation at HOXA10 may be responsible for its aberrant expression in the endometrium of patients with endometriosis. *Am J Obstet Gynecol* 2005;**193**:371–380.

Wu Y, Strawn E, Basir Z, Halverson G, Guo SW. Aberrant expression of deoxyribonucleic acid methyltransferases DNMT1, DNMT3A, and DNMT3B in women with endometriosis. *Fertil Steril* 2007;**87**:24–32.

Xue Q, Lin Z, Cheng YH, Huang CC, Marsh E, Yin P, Milad MP, Confino E, Reierstad S, Innes J *et al.* Promoter methylation regulates estrogen receptor 2 in human endometrium and endometriosis. *Biol Reprod* 2007a;**77**:681–687.

Xue Q, Lin Z, Yin P, Milad MP, Cheng YH, Confino E, Reierstad S, Bulun SE. Transcriptional activation of steroidogenic factor-1 by hypomethylation of the 5′ CpG island in endometriosis. *J Clin Endocrinol Metab* 2007b;**92**:3261–3267.

Submitted on September 3, 2008; resubmitted on November 18, 2008; accepted on January 13, 2009

ANALYTICAL SCIENCES AUGUST 2009, VOL. 25

2009 © The Japan Society for Analytical Chemistry

Notes

Development of Miniaturized Hollow-fiber Assisted Liquid-phase Microextraction with *in situ* Acyl Derivatization Followed by GC-MS for the Determination of Benzophenones in Human Urine Samples

Rie ITO,*† Migaku KAWAGUCHI, Youji KOGANEI,* Hidehiro HONDA,* Noriya OKANOUCHI,* Norihiro SAKUI,*** Koichi SAITO,* and Hiroyuki NAKAZAWA***

**Department of Analytical Chemistry, Faculty of Pharmaceutical Sciences, Hoshi University, 2-4-41 Ebara, Shinagawa, Tokyo 142-8501, Japan*

***Bio-Medical Standard Section, National Metrology Institute of Japan (NMIJ), National Institute of Advanced Industrial Science and Technology (AIST), Tsukuba Central 3, 1-1-1 Umezono, Tsukuba, Ibaraki 305-8563, Japan*

****Agilent Technologies, Hachioji Site, 9-1 Takakura, Hachioji, Tokyo 192-0033, Japan*

A simple and highly sensitive method that involves miniaturized hollow fiber assisted liquid-phase microextraction (HF-LPME) with *in situ* acyl derivatization and GC-MS was developed for the determination of benzophenone (BP) and related compounds in human urine samples. The limits of detection (S/N = 3) and quantification (S/N > 10) of BPs in human urine samples are 0.01 to 0.05 ng ml^{-1} and 0.05 to 0.2 ng ml^{-1}, respectively. The average recoveries of BPs (n = 5) in human urine samples spiked with 10 and 50 ng ml^{-1} BPs are 93.1 to 106.7% (RSD: 1.5 to 8.4%) and 96.3 to 101.5% (RSD: 3.0 to 7.7%), respectively. When the proposed method was applied to human urine samples, BPs were detected at the sub ng ml^{-1} level.

(Received February 20, 2009; Accepted May 21, 2009; Published August 10, 2009)

Introduction

Benzophenone (diphenylmethanone; BP) and related compounds are widely used as chemical sunscreens. They absorb damaging UV rays to decrease the radiation dose, and are widely used in cosmetic products. Benzophenones (BPs) demonstrate maximum absorption at wavelengths of 288 to 290 and 325 nm, and have the property of absorbing wavelengths of 200 to 400 nm. Consequently, BPs are able to absorb UV light that is harmful to the human body in the form of UVA (320 to 400 nm) and UVB (290 to 320 nm), and have been reported to be effective in preventing skin disorders and skin cancer.[1] However, BPs are also suspected to cause pruritus and contact allergies,[2] and to disrupt the endocrine system by exerting estrogenic and anti-androgenic action.[3-5] Recently, the migration of BPs from multilayer plastic-paper materials intended for food packaging and the contamination of food sample with BPs have been reported.[6,7] Due to the widespread usage of BPs, healthy humans may be exposed to BPs *via* a variety of daily activities. Therefore, the assessment of human exposure to BPs is an important task.

It has been reported that when a human ingests BP, it is excreted in urine as a metabolite, such as benzhydrol (BP-OH) glucuronide.[8] Thus, it is thought that human exposure can be evaluated by measuring these compounds in human urine samples. However, as the concentration of BPs in human urine is low, a method with high sensitivity and high accuracy is required.

The determination of BPs in human urine samples has been accomplished with LC with diode array detection,[9] tandem mass spectrometry (MS-MS)[10,11] and GC-MS.[12] However, these techniques require that such pretreatment procedures as liquid-liquid extraction (LLE)[13,14] and solid phase extraction (SPE)[11,15] be performed prior to use, and consume considerable time and labor. As for the time and labor needed for analysis, solid-phase microextraction (SPME) has been successfully used for the determination of BPs in human urine samples.[12] However, because the limit of detection (LOD) of 2-hydroxy-4-methoxybenzophenone (BP-3) is 5 ng ml^{-1}, the sensitivity of the above SPME method remains low. Previously, we reported on a stir bar sorptive extraction (SBSE) method that uses a stir bar coated with polydimethylsiloxane (PDMS) for the determination of BPs in water samples[16,17] and human urine samples.[18] The SBSE method required not only a PDMS-coated stir bar, but also a thermal desorption (TD)-GC-MS system. The TD system had a high running cost because liquid nitrogen was used. To improve the cost performance, liquid-phase microextraction (LPME), solvent microextraction (SME) and a single-drop microextraction (SDME) techniques have been developed.[19-21] LPME consists of extracting and concentrating a target compound with an extremely small amount of extraction solvent using a commercially available microsyringe. Highly sensitive trace analysis is subsequently performed by injecting the extract directly into a GC-MS system using the same microsyringe as that used to collect the extract. The main advantages of these techniques are good cost performance and a wide application

† To whom correspondence should be addressed.
E-mail: rie-ito@hoshi.ac.jp

range that includes polyaromatic hydrocarbons,[22-24] polychlorinated biphenyls (PCBs),[25,26] pesticides,[24,26-29] and organotin compounds.[30] Because of the interfacial activity of urine samples, it is difficult to retain a single droplet on the microsyringe needle tip.[31] Therefore, we have developed miniatulized hollow fiber (HF) assisted LPME for BPs analysis.[32] In that study,[32] five kinds of BPs (BP, BP-OH, 2OH-BP, BP-3, and BP-10) could be analyzed without derivatization. Because of their high polarity and low volatility, phenol compounds including BPs are poorly separated by GC. Derivatization has yielded sharper peaks, and hence better separation of and higher sensitivity for the phenols. However, the derivatization procedure is tedious and time consuming. In order to avoid this problem, *in situ* derivatization was developed. Moreover, with an *in situ* derivatization step, an even wider variety of BP-related compounds could be analyzed to reveal the extent of exposure to BPs.

The aim of this study was to develop an analytical method for the trace analysis of eight kinds of BPs in human urine samples, which employs miniaturized HF-LPME with *in situ* derivatization and GC-MS. The HF-LPME method was performed in conventional 2 ml vials for miniaturization. To consider a further application to valuable samples, such as serum, we performed a miniaturized HF-LPME method.

Experimental

Materials and reagents

Acetonitrile and methanol were purchased from Wako Pure Chemical (Osaka, Japan). BP and deuterium-labeled benzophenone-d_{10} (BP-d_{10}) as surrogate compounds were purchased from Kanto Chemical (Tokyo, Japan). 2,4-Dihydroxybenzophenone (BP-1) and BP-3 were obtained from Sigma-Aldrich (St. Louis, MO). 2-Hydroxy-4-methoxy-4′-methylbenzophenone (BP-10) was obtained from Lancaster Synthesis (Morecambe, England). Benzhydrol (BP-OH), 2-hydroxybenzophenone (2OH-BP), 3-hydroxybenzophenone (3OH-BP), and 4-hydroxybenzophenone (4OH-BP) were purchased from Wako Pure Chemical. *E. coli* β-glucuronidase (25000 U 0.4 ml^{-1}) and *H. pomatia* sulfatase (3650 U ml^{-1}) were purchased from Sigma-Aldrich. Prior to use, β-glucuronidase was added to 0.1 M ammonium acetate to make a total concentration of 10,000 U ml^{-1}. Other reagents and solvents of pesticide or analytical grade were purchased from Wako Pure Chemical (Osaka, Japan). The water purification system was a Milli-Q gradient A 10 with an EDS polisher (Millipore, Bedford, MA).

Concentrated solutions (1.0 mg ml^{-1} in methanol) of BP, BP-OH, 2OH-BP, 3OH-BP, 4OH-BP, BP-1, BP-3, and BP-10 were prepared independently. Then, a mixture-standard solution (10 μg ml^{-1}) was obtained by mixing the concentrated solutions. Urine samples were collected from fourteen healthy volunteers and sample preparation was performed immediately.

Instrumentation

A 10-μl microsyringe for LPME was purchased from SGE Japan (Kanagawa, Japan). The microsyringe needle had a conical tip of 50 mm length and 0.63 mm OD. An accurel Q 3/2 polypropylene hollow-fiber membrane of 600 μm i.d., 200 μm wall thickness, and a 0.2-μm pore size was purchased from Membrana (Wuppertal, Germany). The hollow-fiber membrane was cut manually and carefully into 1.1 cm lengths. Then, the hollow-fiber segments were cleaned in acetone prior to use. For extraction, 2 ml sample vials from Agilent Technologies (Palo Alto, CA) were used.

GC-MS instrument and analytical conditions

GC-MS was performed with an Agilent 6890N gas chromatograph equipped with a 5973N mass-selective detector (Agilent Technologies; Palo Alto, CA). Injection was performed in a pulsed splitless mode and the injection volume was 2 μl. The temperature of the inlet was 250°C. Separation was conducted on a DB-5MS fused silica column (30 m × 0.25 mm i.d., 0.25 μm film thickness, Agilent Technologies). The oven temperature was programmed to increase from 100°C (held for 1 min) to 220°C at 5°C min^{-1}, and then increased to 280°C (held for 3 min) at 15°C min^{-1}. Helium was used as carrier gas at a flow rate of 1.0 ml min^{-1}. The mass spectrometer was operated in the selected ion monitoring (SIM) mode with electron ionization (EI) (ionization voltage: 70 eV). The monitoring ions were as follows: *m/z* 182 and 105 for BP, *m/z* 213 and 256 for acyl-BP-1, *m/z* 227 and 228 for acyl-BP-3, *m/z* 241 and 227 for acyl-BP-10, *m/z* 184 and 105 for BP-OH, *m/z* 197 and 198 for acyl-2OH-BP, *m/z* 198 and 105 for acyl-3OH-BP, and *m/z* 121 and 198 for acyl-4OH-BP. The underlined number is the *m/z* of the ion used for quantification. The monitoring ion for BP-d_{10} was *m/z* 192 as surrogate standard, and quantitative analyses of BPs were performed with a surrogate standard.

Human urine sample preparation by LPME

A human urine sample (1 ml) spiked with surrogate standard was buffered with 1 M ammonium acetate solution (100 μl). After adding β-glucuronidase (10 μl; 10000 U ml^{-1}) and sulfatase (10 μl; 3650 U ml^{-1}), the sample was sealed in a glass tube and gently mixed. Enzymatic de-conjugation to release free BPs was performed by incubating at 37°C for 3 h.[32] Then, a 300-μl aliquot of the de-conjugated sample was transferred to another vial and mixed with the same volume of acetonitrile for deproteination. After shaking sufficiently, it was centrifuged for 10 min at 3000 rpm. Five hundred μl of supernatant was transferred to another vial and 1 ml of purified water was added. Potassium carbonate (1 M K_2CO_3; 50 μl) for a pH adjustment and acetic acid anhydride (20 μl) as a derivatization reagent were added, and the vial was degassed. Then, the sample was agitated. Finally, the sample was subjected to HF-LPME using a 10 μl microsyringe. Before extraction, the microsyringe was rinsed 10 times each with acetone and toluene so as to avoid carryover and air-bubble formation. The needle tip was inserted into a 1.1-cm-long hollow fiber segment. Then, the fiber assembly was immersed in toluene for about 20 s to impregnate its pores with toluene. Toluene in the syringe was injected carefully into the hollow fiber, after which the fiber assembly was completely immersed in the sample solution. LPME was performed at room temperature for 15 min while stirring at 500 rpm. After extraction, 2 μl of the extract was carefully withdrawn into the microsyringe and injected into the GC-MS system.

Results and Discussion

Optimization of extraction solvent and time

The extraction solvent was optimized. Toluene, butyl acetate, and 1-octanol were compared. When toluene was used as the extraction solvent, relatively high responses were obtained for all acyl-BPs. Therefore, toluene was used as the extraction solvent for the HF-LPME method.

One of the most important parameters affecting not only LPME, but also HF-LPME was the extraction time. To

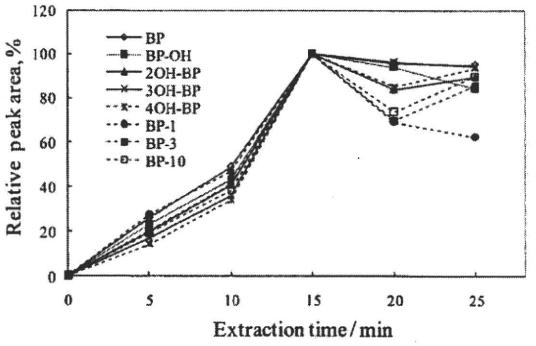

Fig. 1 Extraction time profiles of BPs. Optimum extraction time of analytes in 1 ml standard solutions (5 ng ml^{-1}) using HF-LPME with *in situ* derivatization and GC-MS.

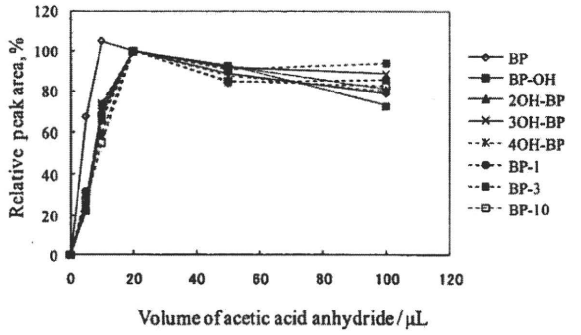

Fig. 2 Optimum volume of acetic acid anhydride for *in situ* derivatization. Optimum volume of acetic acid anhydride for *in situ* derivatization of BPs in 1 ml standard solutions (5 ng ml^{-1}) using HF-LPME with *in situ* derivatization and GC-MS.

determine the optimum extraction time, 5 ng ml^{-1} standard solutions of BPs were used. The extraction time profiles of 1 ml standard solutions of the acyl derivatives of BPs using HF-LPME with in situ derivatization and GC-MS are shown in Fig. 1. The highest response was obtained when the extraction time was 15 min. One possible reason for the decrease in the relative peak area was a reduction in the volume of toluene used as the extraction solvent. We thought that the extraction amounts of analytes were decreased according to the decreasing volume of the extraction solvent. This condition (15 min) was therefore used for the determination of BPs in human urine samples.

Optimization of in situ derivatization and GC-MS conditions

The volumes of K_2CO_3 (5 to 500 μl) and acetic acid anhydride (0 to 50 μl) in the *in situ* derivatization step were optimized. When 50 μl of K_2CO_3 was used for a pH adjustment, all BPs showed relatively high responses. As shown in Fig. 2, the highest response was obtained from BP when 10 μl of acetic acid anhydride was used. When 20 μl of acetic acid anhydride was used for the *in situ* derivatization of BPs, relatively high responses were obtained as well (Fig. 2). Therefore, 20 μl of acetic acid anhydride was used as the optimum volume. We thought that the pH changed when it was added over the 20 μl of acetic acid anhydride.

An EI-MS analysis of the standard solutions of analytes in the scan mode was conducted. Major and minor signals were used

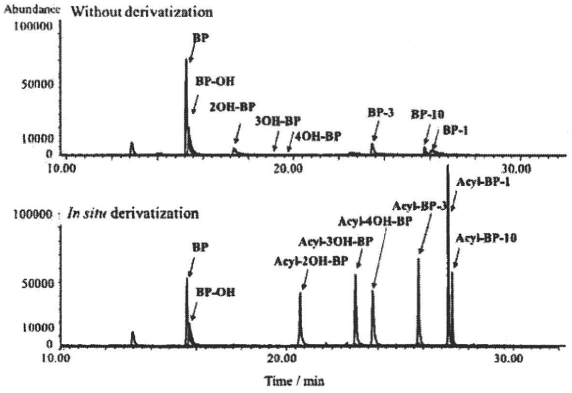

Fig. 3 Comparison of chromatograms of BPs obtained with and without derivatization. For HF-LPME with *in situ* derivatization, derivatization reagents were added to 1 ml of BP standard solution (500 ng ml^{-1}) and the extraction was commenced for 15 min at room temperature in a glass vial. Then, the extraction solvent was subjected to GC-MS analysis. For HF-LPME without *in situ* derivatization, the same procedure was performed, except that no derivatization reagents were added.

as quantification and qualifier ions, respectively. The monitoring ions were as follows: *m/z* 182 and 105 for BP, *m/z* 213 and 256 for acyl-BP-1, *m/z* 227 and 228 for acyl-BP-3, *m/z* 241 and 227 for acyl-BP-10, *m/z* 184 and 105 for BP-OH, *m/z* 197 and 198 for acyl-2OH-BP, *m/z* 198 and 105 for acyl-3OH-BP, and *m/z* 121 and 198 for acyl-4OH-BP.

The effect of *in situ* derivatization was examined. As shown in Fig. 3, peaks of 3OH-BP and 4OH-BP could be detected in the case with *in situ* derivatization. Moreover, the peaks of other acyl-BPs became sharp, since the phenolic hydroxyl group was derivatized. Therefore, *in situ* derivatization was a useful method for the determination of trace levels of BPs in human urine samples.

Analytical figures of merit

The limits of detection (LODs) (signal-noise ratio: $S/N = 3$) and the limits of quantification (LOQs) ($S/N > 10$) of BPs in human urine samples subjected to *in situ* derivatization were 0.01 to 0.05 ng ml^{-1} and 0.05 to 0.2 ng ml^{-1}, respectively. For BP determination, calibration curves were obtained by plotting the peak-area ratio versus the concentration. The calibration curves for analytes were linear with correlation coefficients >0.995 in the range of 0.05 to 100 ng ml^{-1} for BP-3, 0.2 to 100 ng ml^{-1} for BP-OH, and 0.1 to 100 ng ml^{-1} for the other BPs (Table 1). The relative recovery and precision of the method were assessed by replicate analyses ($n = 5$) of human urine samples spiked at 10 and 50 ng ml^{-1}. Non-spiked and spiked samples were subjected to HF-LPME with *in situ* derivatization and GC-MS. Typical chromatograms of spiked urine samples are shown in Fig. 4. The relative recoveries were calculated by subtracting the results for non-spiked samples from those for spiked samples. The results were obtained by using calibration curves of the standard solutions with surrogate standards. The average recoveries of analytes ($n = 5$) in human urine samples spiked with 10 and 50 ng ml^{-1} BPs were 93.1 to 106.7% (RSD: 1.5 to 8.4%) and 96.3 to 101.5% (RSD: 3.0 to 7.7%), respectively (Table 2). Therefore, this method enables precise determinations of standards, and can be applied to the determination of BPs in human urine samples.

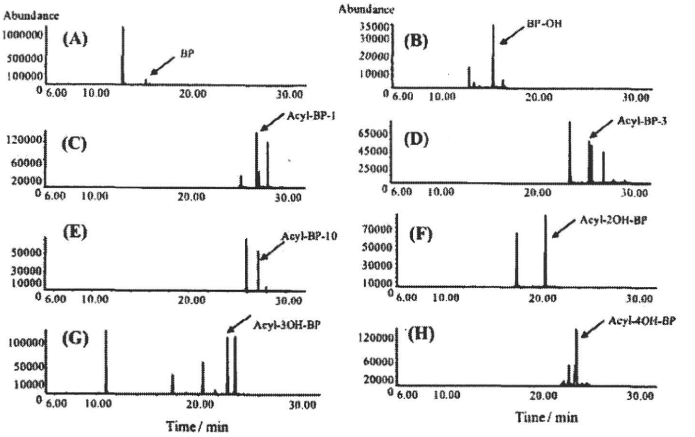

Fig. 4 CTypical chromatograms of spiked urine samples. SIM chromatograms (50 ng ml^{-1} spiked in urine sample) of BP (A), BP-OH (B), acyl-BP-1 (C), acyl-BP-3 (D), acyl-BP-10 (E), acyl-2OH-BP (F), acyl-3OH-BP (G), and acyl-4OH-BP (H) were monitored at *m/z* 182, 184, 213, 227, 241, 197, 198, and 121, respectively.

Table 1 Analytical figures of merit of HF-LPME with *in situ* derivatization and GC-MS

	LOD/ ng ml^{-1}	LOQ/ ng ml^{-1}	Linear range/ ng ml^{-1}	Correlation coefficient, *r*
BP	0.02	0.1	0.1 - 100	0.999
BP-OH	0.05	0.2	0.2 - 100	0.999
2OH-BP	0.02	0.1	0.1 - 100	0.995
3OH-BP	0.02	0.1	0.1 - 100	0.998
4OH-BP	0.02	0.1	0.1 - 100	0.997
BP-1	0.02	0.1	0.1 - 100	0.998
BP-3	0.01	0.05	0.05 - 100	0.996
BP-10	0.02	0.1	0.1 - 100	0.996

LOD, Limit of detection (*S/N* = 3); LOQ, limit of quantification (*S/N* > 10)

Table 2 Recoveries of BPs in human urine samples

	10 ng ml^{-1} spiked		50 ng ml^{-1} spiked	
	Recovery, %	RSD, %	Recovery, %	RSD, %
BP	101.5	5.8	99.5	5.7
BP-OH	97.5	6.0	99.7	3.4
2OH-BP	97.9	1.6	100.8	3.0
3OH-BP	97.9	1.5	100.8	3.9
4OH-BP	97.8	2.1	100.2	4.2
BP-1	106.7	7.7	101.5	3.4
BP-3	93.1	8.4	99.5	4.6
BP-10	95.8	7.6	96.3	7.7

The recoveries and RSD were also examined by replicate analysis (n = 5) of human urine samples.

Table 3 Concentrations of BPs in human urine samples

Volunteer	Concentration of BPs/ng ml^{-1}							
	BP	BP-OH	2OH-BP	3OH-BP	4OH-BP	BP-1	BP-3	BP-10
A	N.D.	0.27	N.D.	N.D.	N.D.	0.32	1.23	N.D.
B	N.D.	0.70	N.D.	N.D.	N.D.	N.D.	0.73	N.D.
C	N.D.	2.48	N.D.	N.D.	N.D.	0.54	1.56	N.D.
D	N.D.	5.16	N.D.	N.D.	N.D.	N.D.	2.59	N.D.
E	N.D.	6.36	N.D.	N.D.	N.D.	N.D.	1.02	N.D.
F	N.D.	4.10	N.D.	N.D.	N.D.	N.D.	0.55	0.56
G	N.D.	10.0	N.D.	N.D.	N.D.	N.D.	0.48	0.71
H	N.D.	2.65	N.D.	N.D.	N.D.	N.D.	0.45	N.D.
I	N.D.	1.37	N.D.	N.D.	N.D.	1.15	4.29	0.94
J	N.D.	0.78	N.D.	N.D.	N.D.	0.75	4.91	N.D.
K	N.D.	0.70	N.D.	N.D.	N.D.	N.D.	0.36	N.D.
L	N.D.	0.94	N.D.	N.D.	N.D.	1.91	1.67	1.07
M	N.D.	2.11	N.D.	N.D.	0.15	3.13	6.91	1.31
N	N.D.	4.14	N.D.	N.D.	N.D.	N.D.	2.25	N.D.

N.D. indicates not determined.

Determination of BPs in human urine samples

Urine samples from fourteen healthy volunteers (five females and nine males) were analyzed using the present method. BP, 2OH-BP and 3OH-BP were not detected in the human urine samples. In contrast, BP-OH and BP-3 were detected in all urine samples in the range of 0.27 to 10.0 ng ml^{-1} and 0.36 to 6.91 ng ml^{-1}, respectively (Table 3). Trace amounts of BP-1, BP-10, and 4OH-BP were detected in some samples.

The Ministry of the Environment has published an annual report, "Chemicals in the Environment, FY2005," which contains the results of an environmental survey and monitoring of chemicals. The Ministry of the Environment has also conducted indoor-air monitoring to determine BPs.[33] The report states that BP and BP-3 were determined frequently in the 68 indoor air samples analyzed. Actually, BP and BP-3 were detected in 67 indoor air samples. Taking the frequent detection of BP-3 into consideration, it was reasonable that BP-3 was detected in all human urine samples. Meanwhile, BP, which was also detected in indoor air samples, was metabolized to BP-OH, which was detected in all human urine samples.

The combination of HF-LPME with *in situ* derivatization and GC-MS led to the successful determination of trace amounts of BPs in human urine samples. We have previously reported on the analysis of BPs in a human urine sample by SBSE-TD-GC-MS.[18] In order to improve the sensitivity and cost performance,